INVESTIGATION OF DOSIMETRIC AND THERMOLUMINESCENCE PROPERTIES OF CaSO$_4$:Dy   (TLD-900) AND SYNTHETIC QUARTZ CRYSTALS

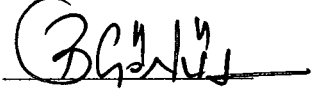M. Sc. Thesis

in

Engineering Physics
University of Gaziantep

BY

VURAL EMİR KAFADAR

JULY 2004

Approval of the Graduate School of Natural and Applied Sciences

Prof.Dr.Bülent GÖNÜL
Director

I certify that this thesis satisfies all the requirements as a thesis

for the degree of Master of Science.

Assoc.Prof.Dr.Zihni ÖZTÜRK
Head of Department

This is to certify that we have read this thesis and that in our
opinion it is fully adequate, in scope and quality, as a thesis for
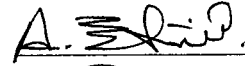the degree of Master of Science.

Assoc.Prof.Dr.Zihni ÖZTÜRK
Supervisor

Examining Committee Members

Assoc.Prof.Dr Zihni ÖZTÜRK

Assoc.Prof.Dr A.Necmeddin YAZICI

Assist.Prof.Dr Metin BEDİR

ABSTRACT

INVESTIGATION OF DOSIMETRIC AND THERMOLUMINESCENCE PROPERTIES OF CaSO$_4$:Dy (TLD-900) AND SYNTHETIC QUARTZ CRYSTALS

KAFADAR Emir Vural

M. SC., in P.E. University of Gaziantep

Supervisor: Assoc.Prof. Dr. Zihni ÖZTÜRK

July 2004, 53 pages

The additive dose (AD), $T_m(E_a)$-T_{stop}, repeated initial rise (RIR), variable heating rate (VHR) and computerized glow curve deconvolution (CGCD) methods were used to determine the number of peaks and kinetic parameters (kinetic orders b, activation energy E_a and attempt-to-escape frequency s) associated with the TL glow peaks in unannealed acid purified synthetic quartz (APSQ) produced by the Fluka company after beta-irradiation between the dose level 0.02 Gy and 2.5 kGy. The E_a-T_{stop} and CGCD methods were indicated that the glow curve of this material is the superposition of at least seven first-order components, which were referred to as P1-P7, in the temperature range between room temperature and 500 °C. The results have indicated that kinetic parameters vary fairly from method to method. The dose responses and fading process, which are very useful in radiation dosimetry and archeological dating, of individual TL peaks of this material were also examined. The dose responses of all peaks have similar pattern, first they follow strong linearity and then saturate at different dose levels. The peaks 1 and 2 were completely

disappeared after one month storage in the dark room at room temperature. On the other hand, the intensity of peak 3 was reduced to 27% of its original value whereas the other peaks (P4-P7) were not sufficiently affected during this period. Additionaly, the glow curve structure of $CaSO_4$ was studied by AD method and it was observed that its glow curve is the superposition of six firs order glow peaks.

ÖZET

SENTETİK KUVARS VE CaSO₄ :Dy (TLD-900) KRİSTALLERİNİN DOZİMETRİK VE TERMOLUMİNESANS ÖZELLİKLERİNİN İNCELENMESİ

KAFADAR Emir Vural

Yüksek Lisans Tezi

Gaziantep Üniversitesi, Fizik Mühendisliği Bölümü

Tez Danışmanı: Doç. Dr Zihni ÖZTÜRK

Temmuz 2004, 53 sayfa

Fluka firması tarafından üretilen ve asitle yıkanmış sentetik kuvars kristalinin 0.02 Gy ile 2.5 kGy arasında beta ışını ile ışınlandıktan sonra, termal ışıldama eğrileri ve bu eğrileri oluşturan ışıldama tepeciklerinin kinetik parametreleri (kinetik derecesi b, aktivasyon enerjisi E_a ve frekans faktörü s), Doz Ekleme (AD), Tekrarlanan İlk Yükselme (RIR), Değişken Isıtma Sıcaklığı Oranı (VHR) ve Bilgisayar ile Işıldama Eğrisi Ayrışımı (CGCD) mètodları kullanılarak bulunmuştur. AD ve CGCD metodları bu materyal'in iç içe geçmiş en az yedi adet birinci dereceden ışıldama tepeciğinden oluştuğunu göstermiştir ve bu tepecikler oda sıcaklığı ile 500 °C arasında P1-P7 olarak belirtilmiştir. Kinetik parametre sonuçları uygulanan metodlara göre değişiklikler göstermektedir. Radyasyon dozimetresinde ve arkeolojik yaş tayinlerinde oldukça kullanışlı olan doz tepkisi eğrisi ve zaman ile sönüm işlemi bu materyal'in her bir tepesi için ayrı ayrı incelenmiştir. Bütün tepeciklerin doz tepkisi aynı modeldedir, öncelikle uygulanan doz miktarı ile çizgisel olarak artar ve ardından farklı dozlarda doyuma ulaşırlar. Birinci ve ikinci ışıldama tepecikleri karanlık bir ortamda bir ay bekletildikten sonra tamamen söndüğü gözlemlenmiştir. Dördüncü, beşinci, altıncı ve yedinci ışıldama tepecikleri bu süreçten etkilenmezken üçüncü tepeciğin şiddeti orjinal değerinin % 27 sine düşmektedir. Bu çalışmada aynı zamanda CaSO₄ : Dy un ışıldama eğrileri doz

ekleme metodu kullanılarak çalışılmıştır. Yapılan deneyler sonrasında bu materyalin iç içe geçmiş birinci dereceden 6 tane ışıldama tepeciğine sahip olduğu gözlenmiştir.

Anahtar kelimeler: termoluminesans, termoluminesans dozimetre, ,TLD, kinetik parametreler, tuzak parametreleri, $CaSO_4:Dy$, APSQ, TLD-900.

ACKNOWLEDGEMENT

TABLE OF CONTENTS

LIST OF FIGURES

LIST OF TABLES

CHAPTER 1

INTRODUCTION

Thermoluminescence is the emission of light from an insulator or semiconductor when it is heated. This is not be confused with the light spontaneously emitted from a substance when it is heated to incandescence. Thermoluminescence is the thermally stimulated emission of light following the previous absorption of energy from radiation [1].

Thermoluminescence (TL) method is a relatively complex process since it involves a trap and a luminescence center. When an insulator or semiconductor is exposed to ionizing radiation at room or at low temperature, electrons are released from the valance band to the conduction band. This leaves a hole in the valance band. Both types of carriers become mobile in their respective bands until they recombine or until they are trapped in lattice imperfections in the crystalline solids. These lattice imperfections play very crucial role in the TL process. The trapped electrons may remain for a long period when the crystals are stored at room temperature. They can be released due to the sufficient energy given to the electron when the crystal is heated. These electrons may move in the crystalline solid until they recombine with suitable recombination centers that contain hole with the emission of TL light. This process of light emission by thermal stimulation from a crystalline solid after irradiations is called as "thermally stimulated process" or simply "thermoluminescence".

In this statement can be found the three essential ingredients necessary for the production of thermoluminesence. Firstly, the material must be an insulator or a semiconductor - metals do not exhibit luminescent properties. Secondly, the material must have at some time absorbed energy during exposure to radiation. Thirdly, the luminescence emission is triggered by heating the material. In addition, there is one important property of thermoluminescence which cannot be inferred from this statement as it stands at present. It is a particular characteristics of thermoluminescence that, once heated to excite the light emission, material can not

be made to emit thermoluminescence again by simply cooling the specimen and reheating. In order to re-exhibit luminesence the material has to be re-exposed to radiation,where upon raising the temperature will once again produce light emission. The fundamental principles which govern the production of thermoluminescence are essentially the same as those which govern all luminescence process, and in this way thermoluminescence is merely one of a large family of luminescence phenomena [1].

Many natural crystals exhibit thermoluminescence (TL) properties that are suitable for TL dating. The use of TL as a dating tool has frequently relied on quartz as the principal dosimeter material [2]. Quartz is essentially formed from the mineral silicon dioxide (SiO_2) and is a very abundant material in ancient ceramic fragments and geological sediments. Therefore, the TL properties of quartz have been studied primarily for archaeological dating applications. [3]. However, there is a slow progress in the application of quartz to general radiation dosimetry due to its complex TL glow curve structure as well as the wide range of different chemical forms in which it occurs. In the past, considerable researches have been carried out to investigate the TL properties of different types of quartz [4-7]. Examples of glow curves from various forms of quartz show great differences in shape. The majority of glow curves for different types of quartz reported in the literature have shown a cluster of peaks at temperatures of ≈60, 80, 100-110, 130, 180, 200-210, 230 and 310, 350 °C. Although a large number of investigations of the TL properties of quartz have been performed, the TL peaks at 100-110, 200-210, and 350 °C were especially well studied [8-9].

The dosimetric characteristics of TL materials mainly depend on the kinetic parameters quantitatively describing the trapping-emitting centers responsible for the TL emission. The determination of the kinetic parameters is therefore an active area of research and various techniques have been developed to derive the parameters from the glow curve. David and colleagues recorded the glow curves from several different natural quartz specimens and emphasized that it is difficult to compare the published TL from different specimens because of differences in heating rates, pre-irradiation treatment, impurity content, method of manufacture, etc. [10]. McKeever has shown in the case of quartz, that all the glow peaks examined, which did not exhibit thermally stimulated conductivity, appeared to follow first-order kinetics [2]. This was supported by a number of studies carried out using the RIR, peak shape (PS), and CGCD methods [11].

As a broad generalization, for quartz, first-order kinetic has been reported in the majority of cases but not exclusively. Some types of quartz exhibit non-first order behavior that may be the result of complex peak overlap [12]. Evidence for second-order kinetics was found in isothermal decay measurements both below and above room temperature [13]. Schwartzman *et al* were unable to determine unique values for the trapping parameters and concluded that general-order kinetics may apply [14]. West and Carter found evidence for mixed first and second-order kinetics in gamma irradiated fused silica fiber optics [15]. Hornyak *et al* found similar evidence of mixed first and second-order kinetics and a distribution of electron activation energies in the high temperature glow peaks in quartz [9]. The great variability presumably reflects the disparate origins of individual samples and it has been reviewed by Prokein and Wagner that the widely differing values of the kinetic parameters originate from different types of quartz [16]. However, Kitis and his colleagues have recently studied the kinetic parameters of synthetic quartz and quartz from various origins and they have shown that the glow curve of synthetic quartz is the superposition of at least 13 first-order glow peaks and the E_a values obtained using different methods for TL peak at 110 °C from various quartz become the limits of experimental errors [17-18]. Therefore, there is neither agreement concerning the published values of the kinetic parameters obtained from different types of quartz nor a consistent progression.

Therefore, the aim of this study is to determine the kinetic parameters, dose response and stability of TL peaks of APSQ and $CaSO_4$ samples developed by Fluka Company. There are various methods for evaluating the kinetic parameters from TL glow curves [19]. When one of the glow peaks is highly isolated from the others, the experimental methods such as initial rise (IR), variable heating rates (VHR), and peak shape (PS) methods are suitable methods to determine these parameters. However as in most TL materials, the glow curve of APSQ consists of several overlapping peaks. When more than one glow peak is present in the glow curve, there are essentially two ways to obtain these parameters: the first way is to isolate each individual TL peak from others using partial thermal annealing treatment and the second way is to make a complete glow curve analysis using deconvolution [20]. The difficulty arises in the first method due to the problems in isolating the peak of interest without any loss of intensity. The major attractive feature of the deconvolution technique is the simultaneous determination of kinetic parameters of

all peaks with no thermal treatment. However, deconvolution method has also its disadvantages over the classical methods in some cases, especially the structure of glow curve is very complex. Therefore, different methods together with deconvolution method have been used to determine the kinetic parameters of APSQ due to some difficulties in interpreting the deconvolution results. These are AD, $T_m(E_a)$-T_{stop}, RIR, VHR, and CGCD methods.

Another material being investigated in this thesis is $CaSO_4$. For large scale and long term dosimetric applications, TL dosimetric systems are superior to photographic emulsion and other dosimetric devices. The TL stability of a phosphor at ambient temperatures is one of the important parameters in dosimetric applications as well [21]. During the last four decades thermoluminescence phosphor $CaSO_4$: Tm and $CaSO_4$: Dy have become widely used detectors in the various fields of radiation dosimetry especially in the precise measurements of small integrated external radiation doses [22]. Calcium Sulphate doped with dysprosium ($CaSO_4$: Dy) is a highly sensitive thermoluminescent (TL) dosimeter material. It is approximately 30 to 50 times more sensitive than TLD – 100. This is especially true for ($CaSO_4$: Dy) exposed to gamma irradiation [23]. Dysprosium activated $CaSO_4$ commercially available as TLD-900 from the Harshaw-Bicron Chemical Co. The prefence for this material is frequently justified by its easy preperation, high sensitivity, and apparently simple glow curve structure. $CaSO_4$:Dy compared to other phosphor shows small fading of the TL dosimetric peak [24]. By several studies it has been demonstrated that the TL glow curve behaviour of $CaSO_4$: Dy and other phosphors is highly dependent on radiation quality and dose. In actual practise of TL applications, there may be a time gap between the irradiations and their corresponding TL measurements. Therefore, a knowledge about the effect of radiation quality and dose on TL stability is definetly desirable [25-26].

An additional significant advantage is that the preperation tecnique is simple so that with proper attention to detail (purity of starting material, doping concentrations etc.), any laboratory equipped with routine facilities can undertake its preperation. The main disadvantage of $CaSO_4$: Dy is of course, its nontissue – equvalent response to low energy gamma rays [23]. More recent research has begun to adress the problem of determining the TL mechanisms involved in this system. There exist a number of the elements that are known as activators of the TL process in $CaSO_4$; of these, manganes (Mn) and dysprosium (Dy) are the most efficient.

However, if activated by Mn^{+2} ions, $CaSO_4$ demonstrates a rapid loss of TL signal at room temperature, referred to as fading. This makes $CaSO_4 : Mn^{+2}$ a somewhat less than desirable dosimeter material for the most practical applications. Since $CaSO_4$ doped with Dy^{+3} ion impruties does not exhibit this fading, the majority of recent research has concentrated on the $CaSO_4 : Dy^{+3}$ system [23]. Glow curve from $CaSO_4$ samples containing different activators show that TL peaks occur more or less at the same temperature, but that the intensities of the peaks change relative to each other when different impurities are present. A number of glow curve studies on $CaSO_4$: Dy have observed a change in the glow peak temperatue of the 200 °C " dosimetric peak" with increasing gamma- irradiation dose [23].

CHAPTER 2

THEORY OF THERMOLUMINESCENCE

2.1. Basic concepts of thermoluminescence in solids

The phenomenon thermoluminescence (TL) has been known for a long time. The first application of this phenomenon for dosimetric purposes was from Daniel et al. [27]. Since then much research has been carried out for a better understanding and improvement of the material characteristics as well as to develop new TL materials. Nowadays, thermoluminescence dosimetry (TLD) is a well-established dosimetric technique with applications in areas such as personnel, environmental and clinical dosimetry.

TLD is based on materials which (after exposure to ionizing radiation) emit light while they are heated. The impurities in the TL material give rise to localized energy levels within the forbidden energy band gap and that these are crucial to the TL process. As a means of detecting the presence of these defect levels, the sensitivity of TL is unrivalled. Townsend and Kelly [28] estimate that the technique is capable of detecting as few as 10^9 defects levels in a specimen. To put this number into perspective one should realize that detectable chemical `purity' in a sample is six orders of magnitude higher. The high sensitivity, allows the determination of very low radiation doses. On the other hand, it handicappes us in investigation into the relation between the luminescence and the defects involved in this process. The sensitivity of thermoluminescent material varies depending on the type of dosimeter.

TL is a luminescence phenomenon of an insulator or semiconductor which can be observed when the solid is thermally stimulated. TL should not be confused with the light spontaneously emitted from a substance when it is heated to incandescence. At higher temperatures (say in excess of 200°C) a solid emits (infra) red radiation of which the intensity increases with increasing temperature. This is thermal or black body radiation. TL, however, is the thermally stimulated emission of light following the previous absorption of energy from radiation. According to this

phenomenon, the three essential ingredients necessary for the production of TL can be deduced. Firstly, the material must be an insulator or semiconductor--metals do not exhibit luminescent properties.

Secondly, the material must have at some time absorbed energy during exposure to ionizing radiation. Thirdly, the luminescence emission is triggered by heating the material [29]. A thermoluminescent material is a material that absorbs some energy which is stored during exposure to ionizing radiation. When the material is heated, the stored energy is released in the form of visible light as seen in Fig.2.1. In fact that TL does not refer to thermal *excitation*, but to *stimulation* of luminescence in a sample which was excited in a different way. TL material can not emit light again by simply cooling the sample and reheating it another time. It should first be re-exposed to ionizing radiation before it produces light again. The storage capacity of a TL material makes it suitable for dosimetric applications.
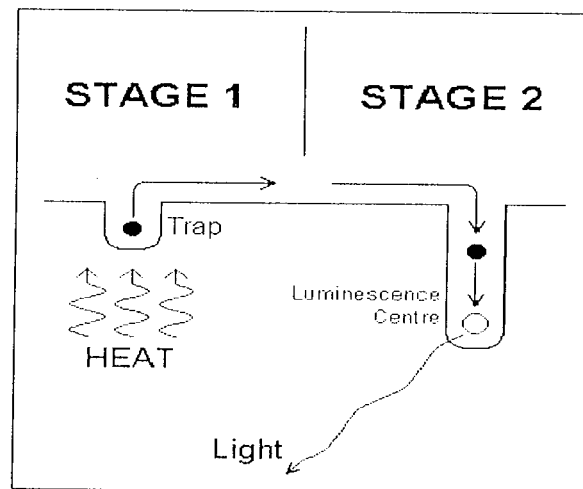
Figure 2.1. Phenomena of thermal excitation of luminescence

2.2. The one trap–one centre model

The energy band theory of solids explains the observed TL properties. In an ideal semiconductor or insulator crystalline most of the electrons reside in the valence band. The next highest band that the electrons can occupy is the conduction band, separated from the valence band by the so-called forbidden band gap. The energy difference between the valence band and conduction band is E_g. However, whenever structural defects occur in a crystal, or if there are impurities within the lattice, there is a possibility for electrons to possess energies which are forbidden in the perfect crystal. In a simple TL model two levels are assumed, one situated below

7

the bottom of the conduction band and the other situated above the top of the valence band (Fig. 2.2). The highest level indicated by T is situated above the equilibrium Fermi level (E_f) and thus empty in the equilibrium state, i.e. before the exposure to radiation and the creation of electrons and holes. It is therefore a potential electron trap. The other level (indicated by R) is a potential hole trap and can function as a recombination centre.

The absorption of radiant energy with $h\gamma > E_g$ results in ionisation of valence electrons, producing energetic electrons and holes which will, after thermalization, produce free electrons in the conduction band and free holes in the valence band (transition a). The free charge carriers recombine with each other or become trapped. In the case of direct recombination an amount of energy will be released which may excite a luminescent centre.
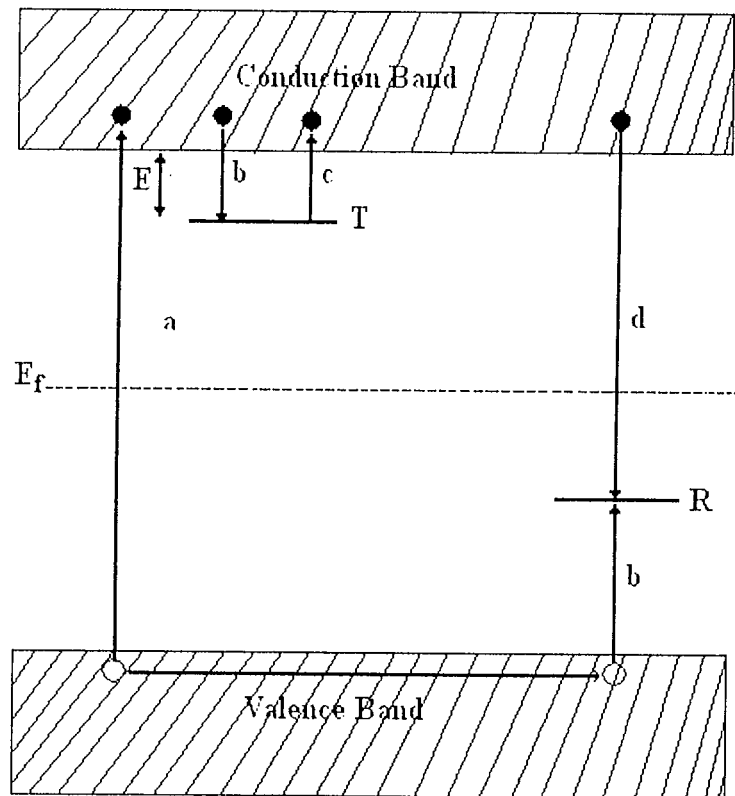
Figure 2.2. Energy band model showing the electronic transitions in a TL material according to a simple two-level model (a) generation of electrons and holes; (b) electron and hole trapping; (c) electron release due to thermal stimulation; (d) recombination. (•) shows electrons, (○) shows holes. Level T is an electron trap, level R is a recombination centre, E_f is Fermi level

8

The luminescent centre relaxes (returns to the ground state) under the emission of light. However, in semiconductors and insulators a certain percentage of the charge carriers is trapped: the electrons at T and the holes at R (transition b). The probability per unit time of release of an electron from the trap is assumed to be described by the Arrhenius equation,

$$p = s \exp\left\{-\frac{E}{kT}\right\} \qquad (2.1)$$

where p is the probability per unit time, s is the frequency factor [30]. In the simple model s is constant, E is called the trap depth or activation energy, the energy needed to release an electron from the trap into the conduction band (see Fig.2.2).

The other symbols have their usual meaning: k is Boltzmann's constant=8.617×10^{-5} eV/K, and T is the absolute temperature. If the trap depth $E>>kT_0$, with T_0 the temperature at irradiation, trapped electrons will remain for a long period of time, until exposure to the radiation there will exist a substantial population of trapped electrons. There must be an equal population of trapped holes at level R, due to the free electrons and holes created and annihilated in pairs. Because the normal equilibrium Fermi level E_f is situated below level T and above level R, these populations of trapped electrons and holes represent a non-equilibrium state. The reaction path for return to equilibrium is always open, but because the perturbation from equilibrium (during exposure to ionising radiation) was performed at low temperature (compared to E/k), the relaxation rate as determined by Eq. 2.1 is slow. Thus, the non-equilibrium state is metastable and will exist for an indefinite period, governed by the rate parameters E and s.

The return to equilibrium can be speeded up by raising the temperature of the TL material above T_0. This will increase the probability of detrapping and the electrons will now be released from the trap into the conduction band. The charge carrier migrates through the conduction band of the crystal until it undergoes recombination at recombination centre R. In the simple model this recombination centre is a luminescent centre where the recombination of the electron and hole leaves the centre in one of the higher excited states. Return to the ground state is coupled with the emission of light quanta, i.e. TL. The intensity of TL $I(t)$ in photons per second at any time t during heating is proportional to the rate of recombination of

9

holes and electrons at R. If m (m^{-3}) is the concentration of holes trapped at R the TL intensity can be written as

$$I(t) = -\frac{dm}{dt} \qquad (2.2)$$

Here we assume that each recombination produces a photon and that all produced photons are detected. The rate of recombination will be proportional to the concentration of free electrons in the conduction band n_c and the concentration of holes m,

$$I(t) = -\frac{dm}{dt} = n_c m A \qquad (2.3a)$$

with the constant A the recombination probability expressed in units of volume per unit time which is assumed to be independent of the temperature.

The rate of change of the concentration of trapped electrons n is equal to the rate of thermal release minus the rate of retrapping,

$$-\frac{dn}{dt} = np - n_c(N-n)A_r \qquad (2.3b)$$

with N the concentration of electron traps and A_r the probability of retrapping (m^3/s). Likewise the rate concentration of free electrons is equal to the rate of thermal release minus the rate of retrapping and the rate of recombination,

$$\frac{dn_c}{dt} = np - n_c(N-n)A_r - n_c m A \qquad (2.3c)$$

Eqs.(2.3a)-(2.3c) described the charge carrier traffic in the case of release of a trapped electron from a single-electron trap and recombination in a single centre. For TL produced by the release of holes the rate equations are similar to Eqs.(2.3a)-(2.3c). These equations form the basis of many analyses of TL phenomena. There is no general analytical solution. To develop an analytical expression some simplifying assumptions must be made. An important assumption is at any time

$$\left|\frac{dn_c}{dt}\right| << \left|\frac{dn}{dt}\right|, \qquad \left|\frac{dn_c}{dt}\right| << \left|\frac{dm}{dt}\right| \qquad (2.4)$$

10

This assumption is called by Chen and McKeever [30] the quasiequilibrium assumption since it requires that the free electron concentration in the conduction band is quasistationary. The trapped electrons and holes are produced in pairs during the irradiation. Charge neutrality dictates therefore

$$n_c + n = m \tag{2.5}$$

which for $n_c \approx 0$ means that $n \approx m$ and

$$I(t) = -\frac{dm}{dt} \approx -\frac{dn}{dt} \tag{2.6}$$

Since $dn_c/dt \approx 0$ one gets from (2.3a) and (2.3b):

$$I(t) = \frac{mAns \exp\left\{-\dfrac{E}{kT}\right\}}{(N-n)A_r + mA} \tag{2.7}$$

2.2.1. First-order kinetics

Even (2.7) cannot be solved analytically without additional simplifying assumptions. Randall and Wilkins [31-32] assumed negligible retrapping during the heating stage, i.e. they assumed $mA >> (N-n)A_r$. Under this assumption Eq.(2.7) can be written

$$I(t) = -\frac{dn}{dt} = sn \exp\left\{-\frac{E}{kT}\right\} \tag{2.8}$$

This differential equation describes the charge transport in the lattice as a first-order process and the glow peaks calculated from this equation are called first-order glow peaks. Solving the differential equation (2.8) yields

$$I(t) = -\frac{dn}{dt} = n_o s \exp\left\{-\frac{E}{kT}\right\} \exp\left\{-s \int_0^t \exp\left\{-\frac{E}{kT(t')}\right\} dt'\right\} \tag{2.9}$$

where n_0 is the total number of trapped electrons at time $t=0$. Usually the temperature is raised as a linear function of time according to

$$T(t) = T_o + \beta t \tag{2.10}$$

with β the constant heating rate and T_0 the temperature at $t=0$. This gives for the intensity as function of temperature

$$I(T) = -\frac{1}{\beta}\frac{dn}{dt} = n_o\frac{s}{\beta}\exp\left\{-\frac{E}{kT}\right\}\exp\left\{-\frac{s}{\beta}\int_{T_o}^{T}\exp\left\{-\frac{E}{kT'}\right\}dT'\right\}$$ (2.11)

This is the well-known Randall–Wilkins first-order expression of a single glow peak. The peak has a characteristic asymmetric shape being wider on the low temperature side than on the high temperature side. On the low temperature side, i.e. in the initial rise of the glow peak, the intensity is dominated by the first exponential ($\exp(-E/kT)$). Thus, if I is plotted as function of $1/T$, a straight line is expected in the initial rise temperature range, with the slope of $-E/k$, from which the activation energy E is readily found.

The properties of the Randall–Wilkins equation are illustrated in Fig.2.3. In Fig.2.3(a) it is shown how $I(T)$ varies if n_0 varies from $n_0=0.25$ m^{-3} till $n_0=2$ m^{-3} while $E=1$ eV, $s=1.0\times10^{12}$ s^{-1} and $\beta=1$ K/s are kept constant. It can be noted that the temperature at the peak maximum, T_m, stays fixed. This is a characteristic of all first-order TL curves. The condition for the maximum can be found by setting $dI/dt=0$ (or, somewhat easier from $d\ln I(T)/dt=0$). From this condition one gets

$$\frac{\beta E}{kT_m^2} = s\exp\left\{-\frac{E}{kT_m}\right\}$$ (2.12)

In this equation n_0 does not appear which shows that T_m does not depend on n_0. From Fig.2.3(a) it can be further seen that not only the peak height at the maximum but each point of the curve is proportional to n_0. In the application in dosimetry n_0 is the parameter of paramount importance since this parameter is proportional to the absorbed dose. It is simple to see that the area under the glow peak is equal to n_0 since

$$\int_0^{\infty}I(t)dt = -\int_0^{\infty}\frac{dn}{dt}dt = -\int_{n_0}^{n_\infty}dn = n_0 - n_\infty$$ (2.13)

and n_∞ is zero for $t\rightarrow\infty$. In Fig.2.3(b) the activation energy E has been varied from 0.8 to 1.2 eV. As E increases the peak shifts to higher temperatures with a decrease in the height and an increase in the width keeping the area (i.e. n_0) constant.

Similar changes can be noticed as s is varied (see Fig.2.3(c)) but now in the opposite way: as s increases the peak shifts to lower temperatures with an increase of the height and a decrease in width. In Fig.2.3(d) the heating rate has been varied. As β increases the peak shifts to higher temperatures while the height decreases and the width increases just as in the case of decreasing s. This can be expected since s and β appear as a ratio s/β in Eq.(2.11). It is worthwhile to note that of the four parameters the activation energy E and the frequency factor s are the main physical parameters. They are called the trapping parameters and are fixed by the properties of the trapping centre. The other two parameters can be chosen by the experimenter by choosing a certain dose (n_0) and by read-out of the signal at a certain heating rate β. Investigation of a new TL material will therefore start with studying the glow peak behaviour under variation of the absorbed dose and the heating rate.

The evaluation of Eqn.(2.11) is hampered by the fact that the integral on the right-hand side is not elementary in the case of linear heating. Chen [33] has shown how the integral can be approximated by asymptotic series. In practical applications it is convenient to describe the glow peak in terms of parameters which are easy to derive experimentally, namely the intensity of peak at the maximum I_m and the temperature at the maximum T_m. Kitis et al. [34] have shown that Eqn.(2.11) can be quite accurately approximated by

$$I(T) = I_m \exp\left[1 + \frac{E}{kT}\frac{T-T_m}{T_m} - \frac{T^2}{T_m^2}\exp\left\{\frac{E}{kT}\frac{T-T_m}{T_m}\right\}(1-\Delta) - \Delta_m \right]$$

(2.14)

with $\Delta=2kT/E$ and $\Delta_m=2kT_m/E$. Recently Pagonis et al.[35] have shown that a Weibull distribution function also accurately describes the first-order TL curve. These expressions may be convenient for peak fitting purposes.

Figure 2.3: Properties of the R–W first-order TL equation, showing: (a) variation with n_0, the concentration of trapped charge carriers after irradiation; (b) the variation with E, the activation energy; (c) the variation with s, the escape frequency; (d) the variation with β, the heating rate. Parameter values: $n_0=1$ m^{-3}; $E=1$ eV; $s=1\times10^{12}$ s^{-1}, $\beta=1$ K/s of which one parameter is varied while the others are kept constant

2.2.2. Second-order kinetics

Garlick and Gibson [36] considered the possibility that retrapping dominates, i.e. $mA<<(N-n)A_r$. Further they assume that the trap is far from saturation, i.e. $N>>n$ and $n=m$. With these assumptions, Eqn.(2.7) becomes

$$I(t) = -\frac{dn}{dt} = s\frac{A}{NA_r}n^2 \exp\left\{-\frac{E}{kT}\right\}$$

(2.15)

We see that now dn/dt is proportional to n^2 which means a second-order reaction. With the additional assumption of equal probabilities of recombination and retrapping, $A=A_r$, integration of Eqn.(2.15) gives

$$I(T) = \frac{n_0^2}{N}\frac{s}{\beta}\exp\left\{-\frac{E}{kT}\right\}\left[1+\frac{n_0 s}{N\beta}\int_{T_0}^{T}\exp\left\{-\frac{E}{kT'}\right\}dT'\right]^{-2}$$

(2.16)

This is the Garlick–Gibson TL equation for second-order kinetics. The main feature of this curve is that it is nearly symmetric, with the high temperature half of the curve slightly broader than the low temperature half. This can be understood from the consideration of the fact that in a second-order reaction significant concentrations of released electrons are retrapped before they recombine, in this way giving rise to a delay in the luminescence emission and spreading out of the emission over a wider temperature range. The initial concentration n_0 appears here not merely as a multiplicative constant as in the first-order case, so that its variation at different dose levels change the shape of the whole curve. This is illustrated in Fig.2.4(a). It is seen that T_m decreases as n_0 increases. It can be derived [37] that the temperature shift can be approximated by

$$T_1 - T_2 \approx T_1 T_2 \frac{k}{E} \ln f \tag{2.17}$$

where T_1 is the temperature of maximum intensity at a certain dose and T_2 the temperature of maximum intensity at f times higher dose. With the parameter values of Fig.2.4(a) the shift is 25 K. When E=1 eV, T_1=400 K and the absorbed dose is increased by a factor 1000, which is easy to realise experimentally, a temperature shift of 77 K can be expected. From Eqn.(2.17) it follows further that for a given increase of the dose the shallower the trap, i.e., the smaller E, the larger the peak shift. Fig.2.4(b) illustrates the variation in size and position of a second-order peak as function of E, in Fig.2.4(c) s function of s/N, and in Fig.2.4(d) as function of the heating rate. The area under the curve is, as in the case of first-order kinetics, proportional to the initial concentration n_0 but the peak height is no longer directly proportional to the peak area, although the deviation is small.
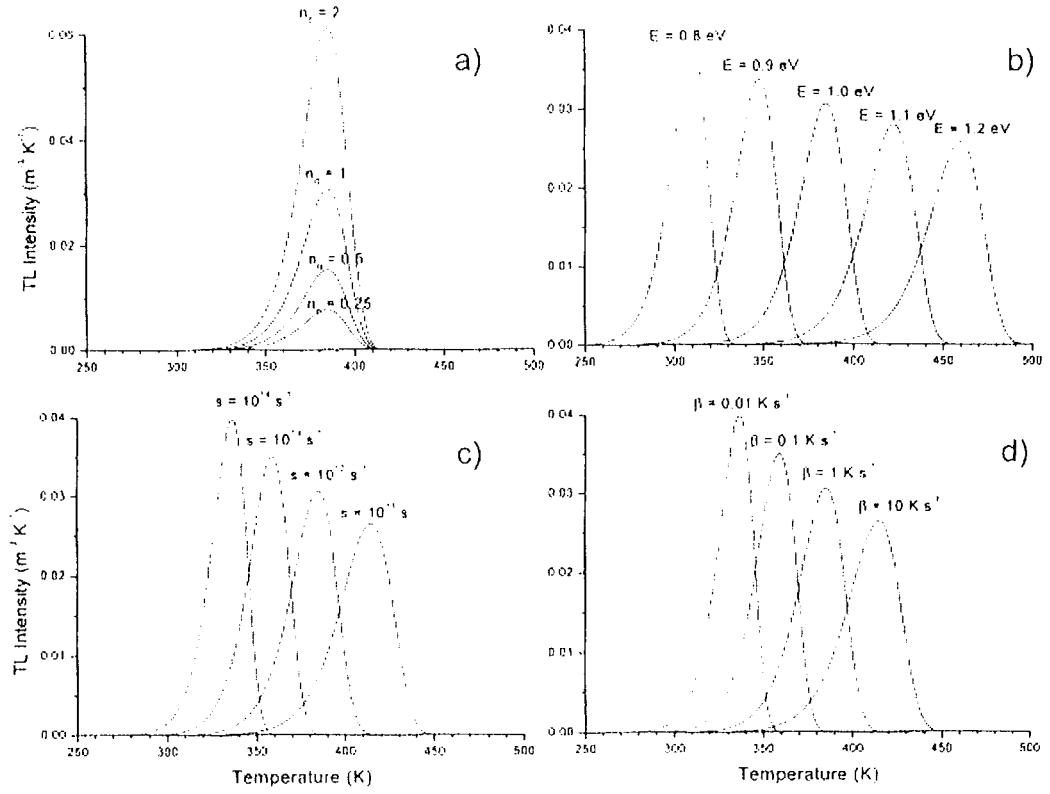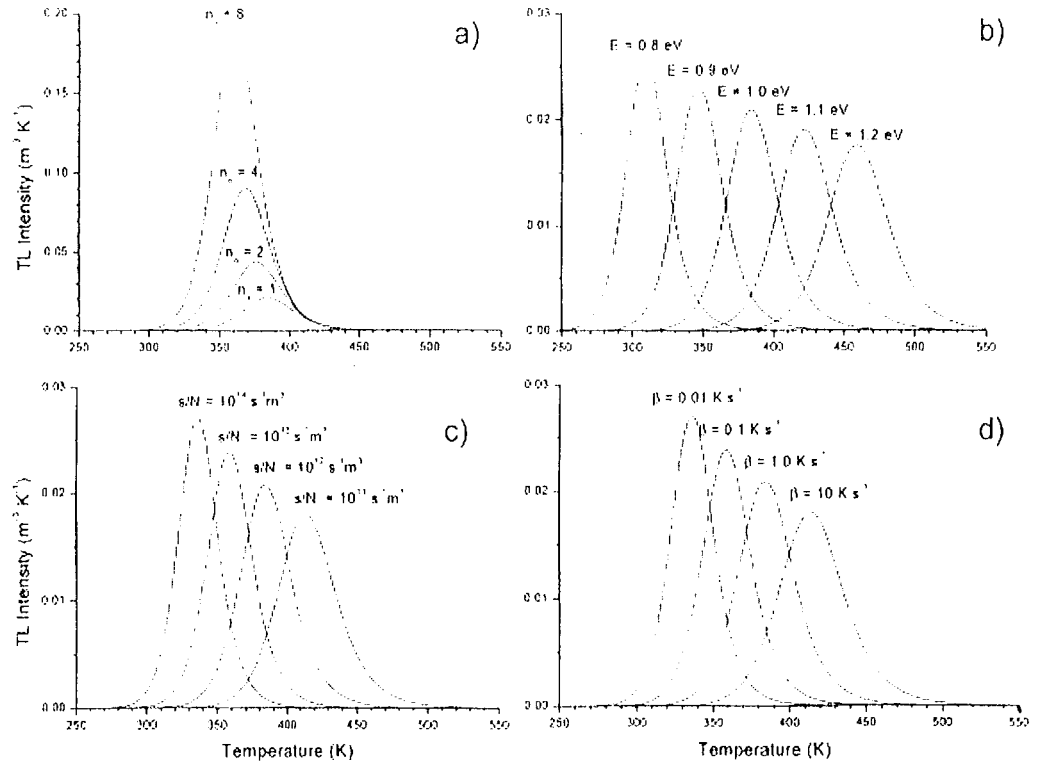
Figure 2.4. Properties of the Garlick–Gibson second-order TL equation, showing: (a) variation with n_0, the concentration of trapped charge carriers after irradiation; (b) the variation with E, the activation energy; (c) the variation with s/N; (d) the variation with β, the heating rate. Parameter values: $n_0=1$ m^{-3}; $E=1$ eV; $s/N=1\times10^{12}$ s^{-1} m^3, $\beta=1$ K/s of which one parameter is varied while the others are kept constant

Note that, similarly to the first-order case, the term dominating the temperature dependence in the initial rise is $\exp(-E/kT)$. So the 'initial rise method' for the determination of the trap depth can be applied here as well.

Also for second-order kinetics the glow peak shape, Eqn.(2.16) can be approximated with a function written in terms of maximum peak intensity I_m and the maximum peak temperature T_m [34]

$$I(T) = 4I_m \exp(\frac{E}{kT}\frac{T-T_m}{T_m}) \times \left[\frac{T^2}{T_m^2}(1-\Delta)\exp\left\{\frac{E}{kT}\frac{T-T_m}{T_m}\right\}+1+\Delta_m\right]^{-2} \quad (2.18)$$

with Δ and Δ_m the same meaning as in Eqn.(2.14).

2.2.3. General-order kinetics

The first- and second-order forms of the TL equation have been derived with the use of specific, simplifying assumptions.

However, when these simplifying assumptions do not hold, the TL peak will fit neither first- nor the second-order kinetics. May and Partridge [38] used for this case an empirical expression for general-order TL kinetics, namely

$$I(t) = -\frac{dn}{dt} = n^b s' \exp\left\{-\frac{E}{kT}\right\}$$ (2.19)

where s' has the dimension of $m^{3(b-1)}$ s^{-1} and b is defined as the general-order parameter and is not necessarily 1 or 2. Integration of Eqn.(2.19) for $b \neq 1$ yields

$$I(T) = \frac{s''}{\beta} n_0 \exp\left\{-\frac{E}{kT}\right\}\left[1 + (b-1)\frac{s''}{\beta}\int_{T_0}^{T}\exp\left\{-\frac{E}{kT'}\right\}dT'\right]^{-b/(b-1)}$$ (2.20)

where now $s''=s'n_0^{b-1}$ with unit s^{-1}. Eqn.(2.20) includes the second-order case ($b=2$) and reduces to Eqn.(2.11) when $b \rightarrow 1$. It should be noted that according to Eqn.(2.19) the dimension of s' should be $m^{3(b-1)}$ s^{-1} that means that the dimension changes with the order b which makes it difficult to interpret physically. Still, the general-order case is useful since intermediate cases can be dealt with and it smoothly goes to first- and second-orders when $b \rightarrow 1$ and $b \rightarrow 2$, respectively (see Fig.2.5).
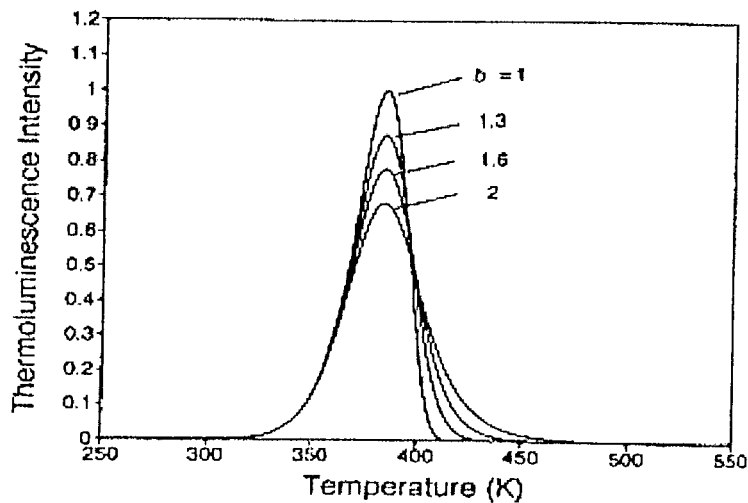
Figure 2.5. Comparison of first-order ($b=1$), second-order ($b=2$) and intermediate-order ($b=1.3$ and 1.6) TL peaks, with $E=1$ eV, $s=1\times10^{12}$ s^{-1}, $n_0=N=1$ m^{-3} and $\beta=1$ K/s (from [34]).

2.2.4 Advanced models

The one trap–one centre model shows all the characteristics of the phenomenon TL and explains the behaviour of the glow peak shape under variation of the dose and heating rate. However, there is no existing TL material known that accurately is described by the simple model. This does not mean that the simple model has no meaning. On the contrary, it can help us in the interpretation of many features which can be considered as variations of the one trap–one centre model. There is no room to discuss all the advanced (more realistic) models in detail. The reader is referred to the text book of Chen and McKeever [30] for a deeper and quantitative treatment. Here, only some models are very briefly mentioned in order to get some idea about the complexity of the phenomenon in a real TL material.

In general, a real TL material will show more than one single electron trap. Not all the traps will be active in the temperature range in which the specimen is heated. A thermally disconnected trap is one which can be filled with electrons during irradiation but which has a trap depth which is much greater than the active trap such that when the specimen is heated only electrons trapped in the active trap (AT) and the shallow trap (ST) (see Fig.2.6(a)) are freed. Electrons trapped in the deeper levels are unaffected and thus this deep electron trap (indicted in Fig.2.6(a) with DET) is said to be thermally disconnected. But its existence has a bearing on the trapping filling and eventually on the shape of the glow peak [40].

In Section 2.1 it was assumed that the trapped electrons are released during heating while the trapped holes are stable in the recombination centre. A description in which the holes are released and recombine at a centre where the electrons are stable during heating is mathematically identical. However, the situation will change if both electrons and holes are released from their traps at the same time at the same temperature interval and the holes are being thermally released from the same centres as are acting as recombination sites for the thermally released electrons and vice versa (see Fig.2.6(b)). In this case Eqn.(2.2) is no longer valid. New differential equations should be drafted. Analysis of this complicated kinetic model reveals a TL glow curve which retains the simple Randall–Wilkins (Eqn.(2.11)) or Garlick–Gibson (Eqn.(2.16)) shape, depending upon the chosen values of the parameters. However, the E and s values used in Eqn.(2.11) and Eqn.(2.16) in order to obtain a fit on this complicated kinetic model need further interpretation.

Another process which might happen is a recombination without a transition of the electron into the conduction band (Fig.2.6(c)) Here the electron is thermally stimulated into an excited state from which a transition into the recombination centre is allowed. This means that the trap has to be in the proximity of a centre.
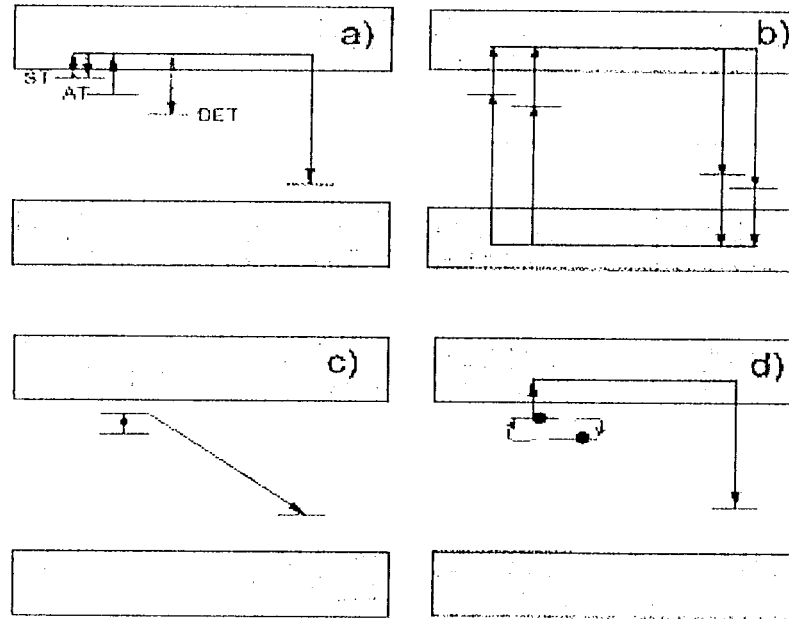
Figure 2.6. Advanced models describing the thermally stimulated release of trapped charged carriers including: (a) a shallow trap (ST), a deep electron trap (DET), and a active trap (AT); (b) two active traps and two recombination centres; (c) localised transitions; (d) defect interaction (trapping centre interacts with another defect).

The transition probability may strongly depend on the distance between the two centres. Under certain assumptions an expression for the TL intensity can be derived [40] which has the same form as Eqn.(2.11) but with s replaced by a quantity related to the probability for recombination. This means that these localised transitions are governed by first-order kinetics.

Finally, we will mention the possibility that the defect which has trapped the electron is not stable but is involved in a reaction with another defect (Fig.2.6(d)). The result may be that at low temperature the trap depth is changing while the trapped electron concentration is stable. At higher temperatures electrons are involved in two processes: the escape to the conduction band and the defect reaction. Piters and Bos [41] have defect reactions incorporated into the rate equations and glow curves simulated. It appears that the simulated glow curves can be very well

19

fitted by Eqn.(2.11) It is clear that (again) the fitting parameters do not have the simple meaning of trap depth and escape frequency.

2.3. Trapping Parameter Determination Methods

The determination of trapping parameters from thermoluminescence glow curves has been a subject of interest for half a century. There are various methods for evaluating the trapping parameters from the glow curves [31-32, 40, 42-46].

When one glow peak is highly isolated from the others, the experimental methods such as initial rise, variable heating rates, isothermally decay, and peak shape methods are suitable methods to determine these parameters. However in most materials, the glow curve consists of several peaks as in the APSQ. In case of overlapping peaks there are essentially two ways to obtain these parameters, the first one is the partial thermal cleaning method and the second one is the computer glow curve deconvolution program. In most cases, the partial thermal cleaning method can not be used to completely isolate the peak of interest without any perturbation on it. Therefore, the computer glow curve deconvolution program has become very popular method to evaluate trapping parameters from TL glow curves in recent years [26].

2.3.1 Peak Shape Method

Evaluation of E from the shape of the peak utilising parameters such as T_m , full width at half-maximum $\omega = T_2 - T_1$, half width on the high temperature side of the maximum $\delta = T_2 - T_m$, half width on the low-temperature side of the maximum $\tau = T_m - T_1$, and $\mu_g = \delta / \omega$ called the shape parameter.

The order of kinetics b can be estimated by means of shape parameters. Chen [42] found that μ_g is not sensitive to changes in E and s, but it changes with the order of kinetics b. It has been shown that the ranges of μ_g varies from 0.42 for $b=1$ to 0.52 for $b=2$ in case of linear heating.

The first peak shape method was developed by Grossweiner [43]; later Chen [42] modified Halperin and Braner's equations [44] for calculating E values;

$$E_\tau = \left[1.51 + 3(\mu_g - 0.42)\right]\frac{kT_m^2}{\tau} - \left[1.58 + 4.2(\mu_g - 0.42)\right]2kT_m$$

$$E_\delta = \left[0.976 + 7.3(\mu_g - 0.42)\right]\frac{kT_m^2}{\delta} \qquad (2.21)$$

$$E_\omega = \left[2.52 + 10.2(\mu_g - 0.42)\right]\frac{kT_m^2}{\omega} - 2kT_m$$

After determination of the activation energy and the order of kinetics, using the following expressions the frequency factor s, it must be noted that this parameter called as pre-exponential factor in the general order kinetic, can be estimated for first and general order kinetics respectively.

$$s = \frac{\beta E}{kT_m^2} \exp\left[\frac{E}{kT_m}\right]$$

$$s = \frac{\beta E}{kT_m^2}\left[\exp(-\frac{E}{kT_m})(1 + (b-1)\frac{2kT_m}{E})\right]^{\frac{b}{b-1}} \qquad (2.22)$$

2.3.2 Isothermal Decay Method

The isothermal decay is quite a different method of analysis of the trapping parameters in which the TL sample temperature is kept constant and the light emission can be recorded as a function of time. Generally, in the isothermal decay method, the following equation is solved for constant T for the first order kinetics

$$I(T) = -c\frac{dn}{dt} = c\frac{n_0}{\tau}\exp(-\frac{t}{\tau}) \qquad (2.23)$$

where n_0 is the initial value of n and $\tau = s^{-1}\exp(\frac{E}{kT})$.

The above equation shows that at a constant temperature T, the light emission will decay exponentially with time t and a plot of $ln(I)$ against t will give a straight line with a slope $m = s\exp(-\frac{E}{kT})$. In order to find E and s, the experiments are carried out at two different constant temperatures T_1 and T_2, resulting in two different slopes m_1 and m_2. Thus the activation energy can be determined by using the following equation

$$E = \frac{k}{(\frac{1}{T_2} - \frac{1}{T_1})} \ln(\frac{m_1}{m_2})$$ (2.24)

The isothermal decay method is not applicable to higher order kinetics. In 1979; a method has been proposed by Kathuria and Sunta [47] to calculate the order of kinetics from the isothermal decay of thermoluminescence. According to this method; if the decaying intensity from the sample is held at a constant temperature, the plot of $I^{(\frac{1}{b}-1)}$ versus t gives a straight line, when the proper value of b is chosen. Therefore, various b values are tried and the correct one is that giving a straight line.

2.3.3 CGCD Method

Computer Glow Curve Deconvolution (CGCD) is one of the most important method to determine trapping parameters from TL glow curves. This method has the advantage over experimental methods in that they can be used in largely overlapping-peak glow curves without resorting to heat treatment

In this study, a CGCD program was used to analyse the glow curve of APSQ. The program was developed at the Reactor Institute at Delft, The Netherlands [48]. This program is capable of simultaneously deconvoluting as many as nine glow peaks from glow curve. Two different models were used in the computer program. In the first model, the glow curve is approximated from first order TL kinetic by the expression,

$$I(T) = n_0 s \ \exp(-\frac{E}{kT})\exp\left[(-\frac{s}{\beta}\frac{kT^2}{E}\exp(-\frac{E}{kT}) * (0.9920 - 1.620\frac{kT}{E_a})\right]$$ (2.25)

In the second model the glow curve is approximated with general order TL kinetics by using the expression,

$$I(T) = n_0 s \ \exp(-\frac{E}{kT})\left[1 + (-\frac{(b-1)s}{\beta}\frac{kT^2}{E}\exp(-\frac{E}{kT}) * (0.9920 - 1.620\frac{kT}{E_a})\right]^{\frac{b}{b-1}}$$ (2.26)

where n_0 (m^{-3}) is the concentration of trapped electrons at $t=0$, s (s^{-1}) is the frequency factor for first-order and the pre-exponential factor for the general-order, E (eV) the

activation energy, T (K) the absolute temperature, k (eVK^{-1}) Boltzmann's constant, β (^{0}Cs^{-1}) heating rate and b the kinetic order.

The summation of overall peaks and background contribution can lead to composite glow curve formula as shown below

$$I(T) = \sum_{i=1}^{n} I_i(T) + a + b\exp(T) \tag{2.27}$$

where $I(T)$ is the fitted total glow curve, a allows for the electronic noise contribution to the planchet and dosimeters infrared contribution to the background.

Starting from the above equation (2.27), the least square minimisation procedure and also FOM (Figure of Merit) was used to judge the fitting results as to whether they are good or not. i.e.

$$FOM = \sum_{i=1}^{n} \frac{|N_i(T) - I(T)|}{A} = \sum_{i=1}^{n} \frac{|\Delta N_i|}{A} \tag{2.28}$$

where $N_i(T)$ is the i-th experimental points (total n=200 data points), $I(T)$ is the i-th fitted points, and A is the integrated area of the fitted glow curve.

From many experiences [49-50], it can be said that if the values of the FOM are between 0.0% and 2.5% the fit is good, 2.5 % and 3.5% the fit is fair, and > 3.5% it is bad fit.

To have a graphic representation of the agreement between the experimental and fitted glow curves, the computer program also plots the function,

$$X(T) = \frac{N_i(T) - I_i(T)}{\sqrt{I_i(T)}} \tag{2.29}$$

which is a normal variable with an expected value 0 and $\sigma=1$ where $\sigma^2(T)=I_i(T)$.

2.3.4. Initial Rise Method

The simplest, and most generally applicable method for evaluating the activation energy E of a single TL peak is the initial rise method. The basic premise upon which this method is based is that at the low temperature end of the peak,all the relevant occupancies of the states, the trap, the recombination center and, in some cases, other interactive states can be considered as being approximately constant.

The rise of the measured intensity as a function of temperature in this region is, therefore, very close to exponential, thus

$$I(T) = C \exp(-E/kT) \qquad (2.30)$$

where the constant C includes all the dependencies on the other parameters and occupancies, E is the activation energy (eV), k is the Boltzmann's constant (eV/K^{-1}) and T is the temperature (K).

Plotting $\ln(I)$ against $1/T$ a linear plot is obtained with slope equal to $-E/k$. Hence it is possible to evaluate E without any knowledge of the frequency factor s by means of equation

$$E = -kd(\ln(I))/d(1/T) \qquad (2.31)$$

Once the value of E was determined, the frequency factor (s) was obtained from the equation

$$\frac{\beta E}{kT_m} = s \exp(-\frac{E}{kT}) \qquad (2.32)$$

where T_m is the temperature at the maximum intensity. This method can only be used when the glow peak is well defined and clearly seperated from the other peaks.

2.3.5. Heating Rate Method

Another important method is various heating rates for the determination of activation energies. If a sample is heated at two different linear heating rates β_1 and β_2 the peak temperatures will be different. Equation (2.32) can therefore, be written for each heating rate and dividing the equation for β_1 (and T_{m1}) by the equation for β_2 (and T_{m2}) and rearranging, one gets an explicit equation for the calculation of E

$$E = k \frac{T_{m1} T_{m2}}{T_{m1} - T_{m2}} \ln[(\frac{\beta_1}{\beta_2})(\frac{T_{m2}}{T_{m1}})^2] \qquad (2.33)$$

The major advantage of the heating rate method is that it only requires data to be taken at a peak maximum (T_m, I_m) which, in case of a large peak surrounded by smaller satellites, can be reasonably accurately determined from the glow curve. Furthermore the calculation of E is not affected by problems due to thermal quenching, as with the initial rise method.

24

When various heating rates for the first-order kinetics are used, the following expression is obtained:

$$\ln(\frac{T_m^{\;2}}{\beta}) = (\frac{E}{k})(\frac{1}{Tm}) + cons\tan t \tag{2.34}$$

A plot of ln $(T_m^{\;2}/\beta)$ versus $(1/\;T_m)$ should yield a straight line with a slope E/k, then E is found. Additionally, extrapolating to $1/T_m = 0$, a value for $ln(sk/E)$ is obtained from which s can be calculated by inserting the value of E/k found from the slope.

This method of various heating rates are applicable for general-order kinetics which includes the second-order case. For the general order case, one can plot $ln\left[I_m^{\;b-1}(T_m^{\;2} / \beta)^b\right]$ versus $1/T_m$, whose slope is equal to E/k.

CHAPTER 3

Experimental Procedure

The materials, equipments and experimental procedures utilized in this work are described below.

3.1. Materials

The samples used in this study were $CaSO_4:Dy$ (TLD-900) crystal chips (the thickness of the sample is 0.40 mm and the diameter is 12 mm) and Quartz crystals (in the form of powder) obtained from Fluka Company.

3.2. Equipments

3.2.1 Radiation Source and Irradiation Procedure

The samples were irradiated at room temperature immediately after quenching. Quartz crystals were irrradiated with ^{90}Sr-^{90}Y β-source and $CaSO_4$ samples were irradiated with Cs-137 gamma source.The activity of β-source is about 100 mCi. It is calibrated by manufacturer on March, 10, 1994. The recommended working life-time is about 15 years. Stronium-90 emits high energy beta particles from their daughter products (^{90}Sr β-0.546 MeV together with ^{90}Y β-2.27 MeV). Beta radiation is absorbed by air, so its intensity declines with distance much more rapidly than inverse square law calculations would indicate. The maximum range of Y-90 beta particles in air is approximately 9 meter. The typical strength of a 100 mCi Sr-90 β-source installed in a 9010 Optical Dating System is 2.64 Gy/minute=0.0438 Gy/Sec for fine grains on aluminium, or 3.3 Gy/min=0.055 Gy/sec for 100 m quartz on stainless still. The irradiation equipment is an additional part of the 9010 Optical Dating System which is purchased from Little More Scientific Engineering, UK [51]. The irradiation source equipment is interfaced to a PC computer using a serial RS-232 port. Quartz crystals were irradiated to various dose levels between ≈0.1 Gy and ≈110 Gy during the variable dose method. The activity of gamma source used for the irradiation of $CaSO_4$ samples is about 100 mGy/hour.

3.2.2 TL Analyzer and TL Measurements

The glow curve measurements for quartz crystals were made using a Harshaw TLD System 3500 Manual TL Reader [52]. It economically provides high reliability. The technical architecture of the system includes both the Reader and a DOS-based IBM-compatible computer connected through a standard RS-232 serial communication port to control the 3500 Reader. The basic block diagram of reader is shown in figure 3.1. All functions are divided between the reader and the specialized TLDShell software that runs on the PC. All data storage, instrument control, and operator inputs are performed on the PC. Signal acquisition and conditioning are performed in the reader. In this way, each glow curve can be analyzed using a best-fit computer program based on a Marquardt algorithm minimisation procedure, associated to first-order and general-order kinetic expressions. The program resolves the individual peaks present in the curve, giving the best values for the different peak parameters.The instrument includes a sample change drawer for inserting and removing the TLD elements. The reader uses contact heating with a closed loop feedback system that produces adjustable linearly ramped temperatures from 1 °C to 50 °C per second accurate to within ± 1 °C to 600 °C in the standard reader.

The Time Temperature Profile (TTP) is user defined in three segments: Preheat, Acquire, and Anneal, each with independent times (Pre-read anneal: adjustable 0 to 1000 sec, Linear ramp: adjustable from 1 °C to 50 °C per second, Post-read anneal: 0 to 1000 sec) and temperature (Pre-read anneal:room temperature to 200 °C, Post-read anneal: up to 400 °C). The typical time temperature profile is shown in figure 3.2. To improve the accuracy of low-exposure readings and to extend planchet life, the 3500 provides for nitrogen to flow around the planchet. By eliminating oxygen in the planchet area, the nitrogen flow eliminates the unwanted oxygen-induced TL signal. Nitrogen is also routed through the photo-multiplier tube (PMT) chamber to eliminate moisture caused by condensation. Glow curves were measured using a platinum planchet at a linear heating rate of 1 °C/s. The time duration between irradiation and necessary TL operation was always kept constant at about 1 min, except for the storage time experiment. For the variable heating rate method heating rates were varied from 1 to 7 °C/s. At each heating rate four chips were read out.

Each chip was read out twice and the second readout is considered to be background of the reader plus chip and was subtracted from the first one and all of the analyses have been carried out after subtraction operations
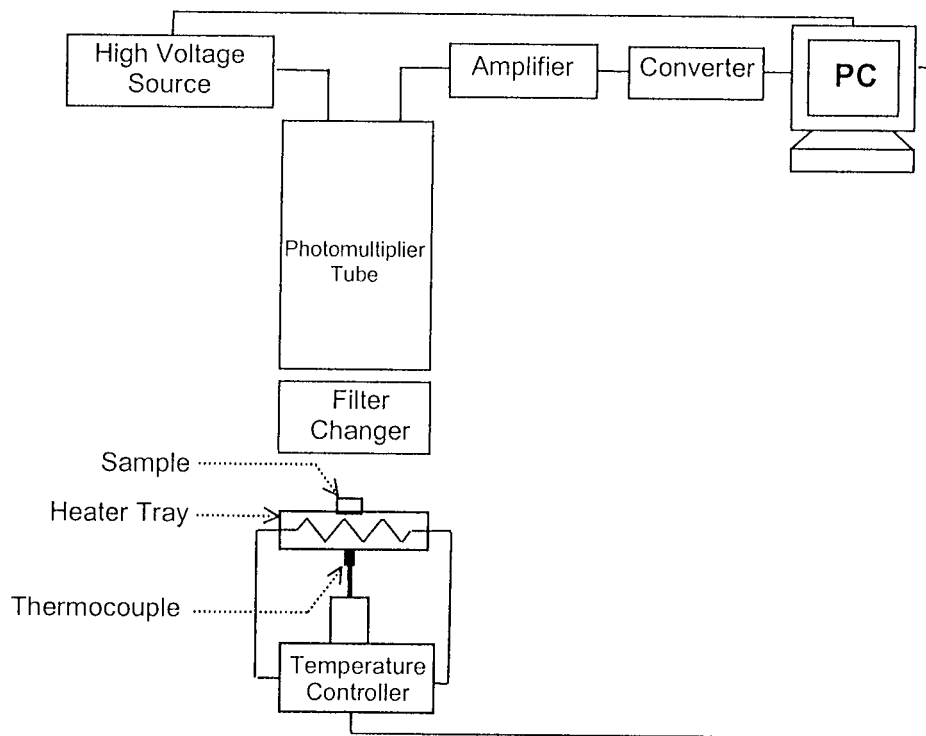

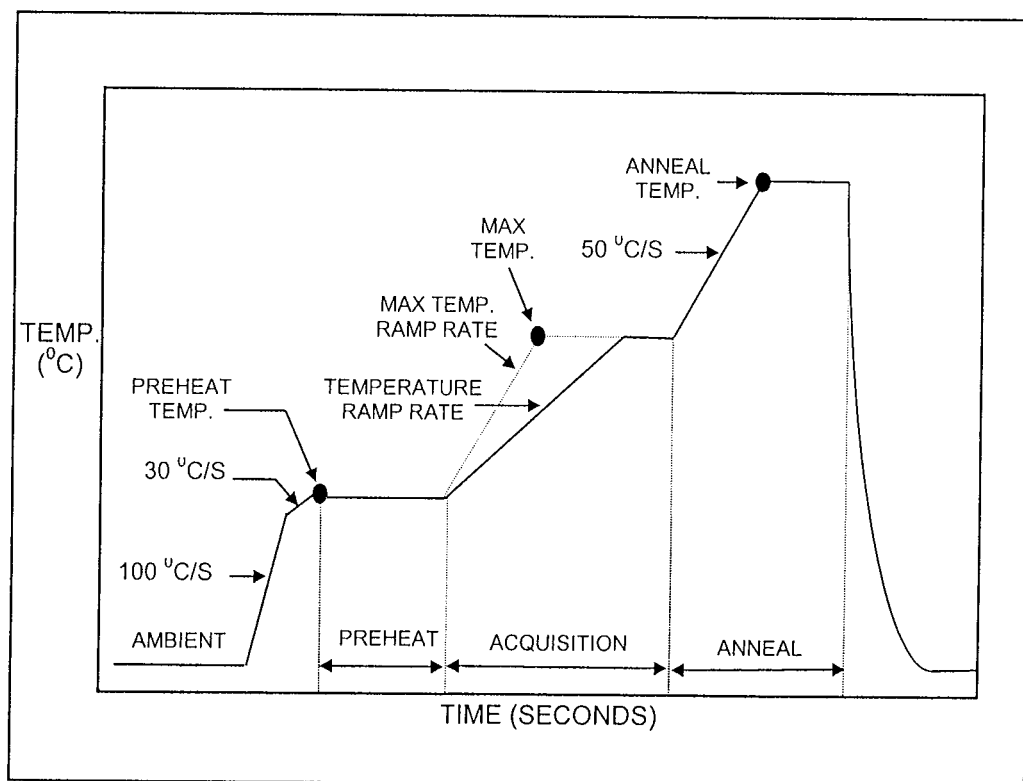Figure 3.1. Basic block diagram of TL reader

Figure 3.2. Typical time temperature profile (TTP)

3.3 Experimental Procedure for APSQ

The acid purified synthetic quartz samples used in this study were in the form of powder that produced from Fluka Company. The extended specifications of this sample are given in Table 3.1.

The samples were first heated up to 500 °C to erase any residual information before the subsequent irradiation and then quickly cooled in air to room temperature. The samples were irradiated at room temperature with beta rays from a calibrated ^{90}Sr-^{90}Y source. The irradiated samples were read out in N_2 atmosphere with a Harshaw QS 3500 manual type reader that is interfaced to a PC where the TL signals were studied and analyzed. Glow curves were measured using a platinum planchet at a linear heating rate of 1 °C/s. In a contact heating, the temperature control is achieved with the temperature of the heating element (planchet) and therefore a thermal lag exists between samples and heater at the high heating rates (>2 °C/s). Five milligrams of powder were used for each measurement and poured onto the planchet as a layer through a vibrating dispenser and it can be assumed that the temperature distribution inside the sample is homogenous. A standard clean glass filter was always installed in the reader between sample and photomultiplier tube. This filter allows the light whose wavelength between ≈250 nm and ≈1000 nm to pass through it and thereupon eliminates unwanted infrared lights that are emitted from heater. The time duration between irradiation and TL reading was always kept constant at about 1 min. For the VHR method, the heating rates were varied from 1 to 5 °C/s. At each experimental measurement, four samples were read out and each sample was read out twice. The second readout is considered to be the background of the reader plus sample; this was subtracted from the first one and all of the analyses have been carried out after the subtraction.

To evaluate the fading in the intensity of APSQ, the samples were firstly irradiated at room temperature up to 50 Gy and then they were stored in the dark room at room temperature.

Table 3.1: Extended Specifications of
acid purified synthetic quartz (APSQ)

Loss on	≤0.1%, 900 °C
particle size	40-100 mesh
Chloride (Cl)	≤50 mg/kg
Ca	≤50 mg/kg
Cd	≤50 mg/kg
Co	≤50 mg/kg
Cu	≤50 mg/kg
Fe	≤100 mg/kg
K	≤500 mg/kg
Na	≤100 mg/kg
Ni	≤50 mg/kg
Pb	≤50 mg/kg
Zn	≤50 mg/kg

3.4 Experimental Procedure for $CaSO_4$

Because Harshaw TLD analyser was out of order and could not be repaired during the preparation time of this thesis $CaSO_4$ samples were analysed by Toledo TLD reader in Ankara Nuclear Research and Training Center (ANAEM). This device allows only reading for different dose levels at a constant heating rate of 1.2 °C/s.

The samples were irradiated at room temperature with gamma rays from a calibrated ^{137}Cs source. The irradiated samples were read out in N_2 atmosphere with a Toledo manual type reader that is interfaced to a X-Y recorder where the TL signals were studied and analyzed. Glow curves were measured using a platinum planchet at a linear heating rate of 1.2 °C/s.

CHAPTER 4

EXPERIMENTAL RESULTS

4.1. Results and discussion for APSQ

The determination of E_a and s mainly depends on the prior knowledge of b and exact number of glow peaks in the glow curve [53]. Therefore, to form an opinion about the b of each individual glow peak, the AD method was firstly used in this thesis. The samples were irradiated at different doses between 0.02 Gy and 2.5 kGy to check the dose dependence effect on the peak positions. This is a simple test for the first-order kinetics. Some of the selected glow curves after different dose levels are shown in Fig.4.1. In TL theory, the peak temperatures of glow peaks are expected to change only with heating rate for $b=1$. Hence, for a constant heating rate, the peak maximum should not be affected by other experimental parameters and should thus be fairly constant within the limit of experimental errors. However, for $b \neq 1$ and below the trap saturation points $\{n_o$ (concentration of trapped electrons)$<N_t$ (concentration of traps)$\}$, the peak temperatures are shifted to the lower temperature side with increasing dose levels. As seen from Fig. 4.1, there is no significant change in the position of peak temperatures and they are within the experimental error ± 3 $^\circ$C for all the doses. This point clearly indicates that the all peaks in the glow curve of APSQ should have first-order kinetics. The number of glow peaks and their kinetic orders were also tested using the RIR method. A strong overlapping of TL peaks makes this method the most suitable procedure for the determination of number of glow peaks and their related kinetic parameters.

Here, an irradiated sample is heated at a linear heating rate up to a temperature T_{stop} corresponding to a point on the low temperature tail of the first peak.
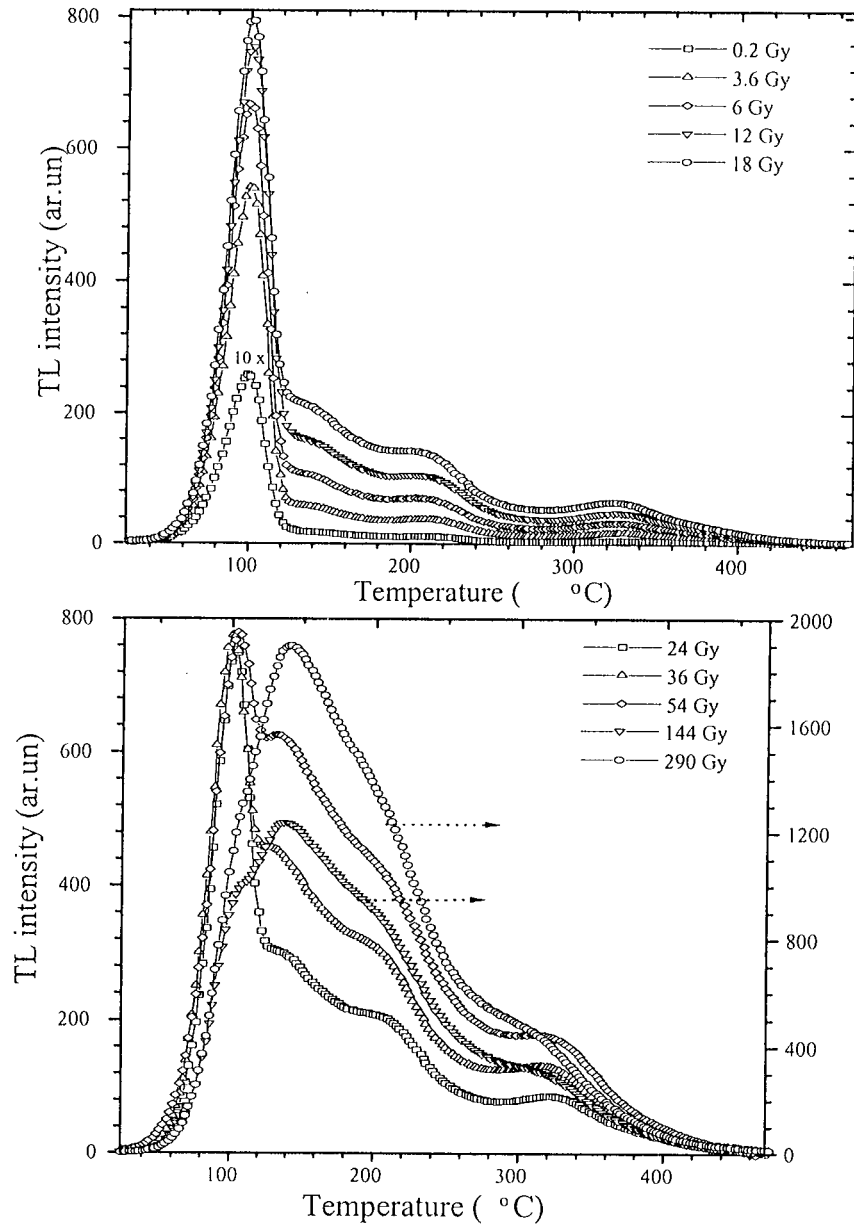

Figure 4.1. The glow curve of APSQ measured after various radiation doses (β=1 °C/s). In all figures, O represents the experimental points

The sample is then cooled down quickly to room temperature and then re-heated at the same rate to record all of the remaining glow curve, and the value of activation energy E_a is calculated. The process is repeated several times on the same

annealed/irradiated sample at a different T_{stop} values, and two measurements were taken within each 10 °C region. According to this method, at the beginning of the TL glow peak, the concentration of trapped electrons n_o changes by only a small amount with temperature and thus it can be regarded as constant, so that the first- and general-order TL equations are simplified as $I(T) \propto A\exp(-E_a/kT)$, where A is a constant and the TL intensity is independent of the b.

Therefore, a plot of $ln(I)$ versus $1/T$ would yield a straight line with a slope of $-E_a/k$ and a y intercept of $ln(s/\beta)$, from which E_a and s can readily be calculated. This method can be used only in the initial region of the TL signal up to ~10% of its peak maximum (I_m). However, if the intensity at the beginning of each peak is very low and especially when the glow curve is composed of several glow peaks, the obtained values of E_a may not reflect the actual values. Therefore, in this case, the values of E_a obtained by the RIR method often need corrections. Christodoulides [54] and S.C.Singh et al. [55] have proposed to use the high-level of glow peaks to reduce the inaccuracies in E_a due to high levels of the used signal, which was also used in the present work. Another matter during the evaluation of E_a by RIR is the effect of thermal quenching on the evaluated E_a. This effect leads to underestimations of the activation energies obtained by RIR method. Since, the experimental glow curve shape is highly distributed by thermal quenching effect, it can't give reliable information about the values of E_a.

However, the RIR method analyzes only that the leading part of the glow peak and as such is yielding data appropriate to only that component of the TL signal comprising the full peak. Therefore, even if the RIR method gives erroneous values of E_a when the thermal quenching is present in the material, it should be expected that the plot of E_a against T_{stop} still gives plateau regions with a gradual decrease at

the end of each plateau after RIR method even if the glow curve is the superposition of overlapping glow peaks. If a plot of E_a against T_{stop} shows a stepwise curve after the RIR method, it allows one to estimate the number of peaks. Each plateau region in this plot indicates the existence of an individual glow peak. If a gradual rise of E_a exists at the end of the plateau region, it is an indication that the glow curve has overlapping glow peaks. Figure 4.2 shows some of the selected glow curves after the $T_m(E_a)$-T_{stop} procedure following the irradiation of samples to a dose level $D=50$ Gy. As seen from this figure, the T_m of all glow peaks is continuously shifted to high temperature side with increasing T_{stop}. The result of calculated activation energies is shown in figure 4.3 as a function of T_{stop}. As shown from this figure, there are at least seven plateau regions, so the RIR studies have identified at least seven peaks in APSQ, designated P1-P7, in the temperature range from ~50-470 °C. The first plateau region between 60 and 120 °C becomes nearly constant around 0.90±0.01 eV which is believed to give the activation energy of first glow peak (P1). After the complete disappearance of peak 1 above $T_{stop}>120$ °C, the calculated activation energies were slightly increased and become constant near 0.93±0.01 eV which is considered to be belonging to peak 2 up to 160 °C. Beyond 160 °C, after a slow increase, the E_a values again become constant near 0.99±0.01 eV which give the E_a value of peak 3 up to 180 °C. At the end of smoothly flat region of peak 3, the calculated activation energies start to increase and reach to 1.11±0.02 eV at 180 °C. This flat region can be considered to provide the E_a value of peak 4. After the complete depletion of peak 4, the calculated value of E_a starts to increase and reaches to another flat region near 1.22±0.02 eV up to 290 °C.
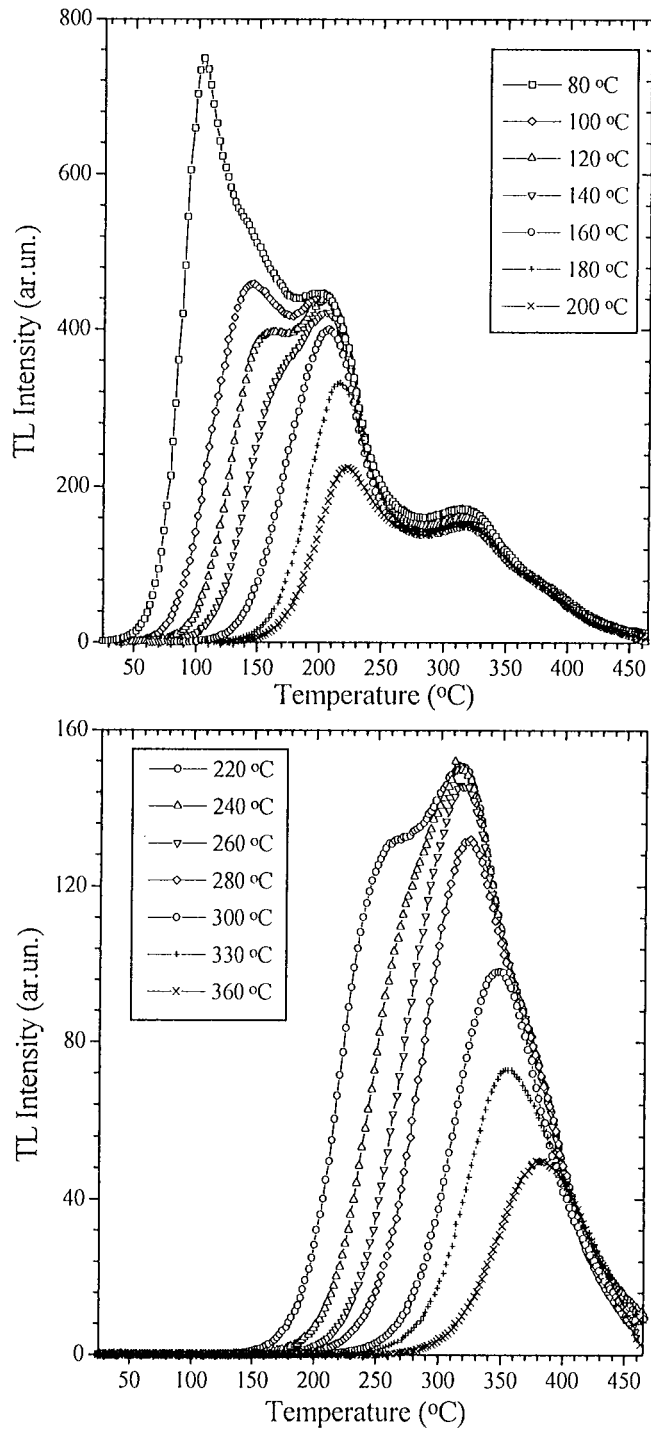
Figure 4.2: Some of the selected glow curves of APSQ after different T_{stop} temperatures at a heating rate $\beta=1$ °C/s. Dose levels are always adjusted to ≈ 50 Gy

This flat region was considered to be corresponding to peak 5. At the end of this region, another flat region was again obtained near 1.28±0.01 eV up to 310 °C, which gives the activation energy of peak 6. When this peak completely disappears, the calculated activation energies are quickly increased from 1.28 to 1.36±0.02 eV up to 330 °C, which is related to peak 7. Finally, when the peak 7 is completely disappeared from the glow curve of this sample around 340 °C, the calculated values of activation energies have continuously increased with increasing stopping temperatures. No any flat regions were noticed above 340 °C.

Figure 4.3: The activation energy (E_a) resulting from the RIR method after $T_m(E_a)$-T_{stop} procedure. Note that each experimental point is the average of at least four measurements

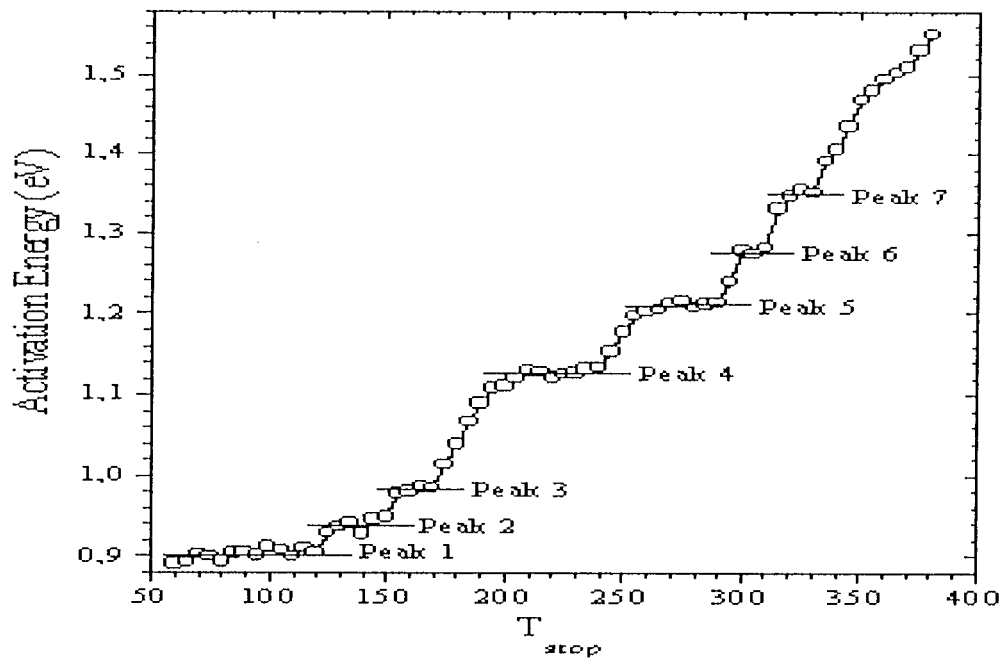Another method that was used to determine the kinetic parameters in the present work is the VHR method. This method is based on the shift position of the temperature at the maximum (T_m) to higher temperatures when the heating rate is increased. In the absence of a distribution of activation energies, a plotting of $ln(T_m^2/\beta)$ against $1/(kT_m)$ should give a straight line of slope E_a/k and intercept $ln(sk/E_a)$.

The major advantage of this method is that the required data is to be taken at a peak maximum (I_m, T_m) which, in the case of a large peak surrounded by smaller satellites, can be reasonably accurately determined from the glow curve. But, a difficulty arises in the case of highly overlapping peaks with comparable intensities, since the local maximums of some glow peaks in the glow curve are not evident. This problem was overcome by deconvolution of glow curves with computer program. In this respect, the peak temperatures of peaks 1, 4 and 5 are easily distinguishable from other peaks and, thereupon, the activation energies of these peaks were calculated by VHR method after determination of their peak temperatures by choosing their local maximums from glow curves. The activation energies of other peaks were determined after the determination of their peak temperatures by CGCD method. A set of measured glow curves at different heating rates after normalization is shown in Fig.4.4. Another important point that has to be taken into consideration to avoid large errors in the kinetic parameters determined by VHR method is the temperature lag (TLA) between the heating element and the thermoluminescent sample during the TL readout in readers using contact heating. To avoid this problem, a simple method recently has been proposed by Kitis and Tuyn [55] to correct the TLA and to determine the exact peak temperatures after different heating rates by using the following equation;

$$T_m^j = T_m^i - C \ln\left(\frac{\beta_i}{\beta_j}\right) \qquad (4.1)$$

where T_m^j and T_m^i are the maximum temperatures of a glow peak with heating rates β_j

and β_i, respectively and C is a constant, which is initially evaluated by using two

very low heating rates where the TLA can be considered as negligible. In preference,

the low heating rates should be chosen below 1 °C/s to calculate the constant C. On

the other hand, the used TLD reader in the present work does not give permission to

low heating rates below 1 °C/s, therefore, two intermediate heating rates 1 and 2 °C/s

were used to calculate constant C and then correct peak temperatures by TLA. The

curves in Fig.4.5 are corresponded to the peak maximum positions corrected for the

TLA and experimental points. As seen from the figure, there are slight differences

between the slopes, each one giving a different trap depth. The calculated kinetic

parameters from the slopes and intercepts are given in Table 4.1.
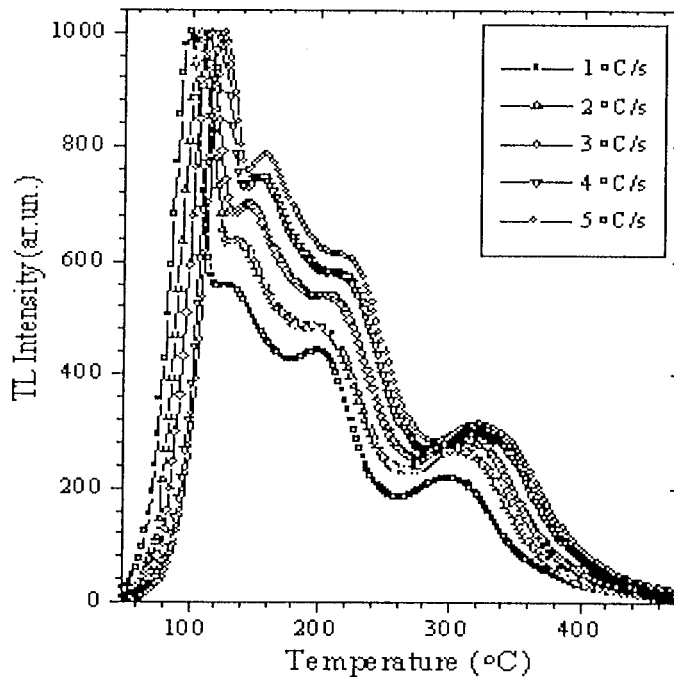

Figure 4.4: Some of the selected and normalized glow curves of TLD-200 measured at various heating rates from 1 °C/s to 5 °C/s. The glow curves were measured after irradiation of samples to a dose level of 50 Gy
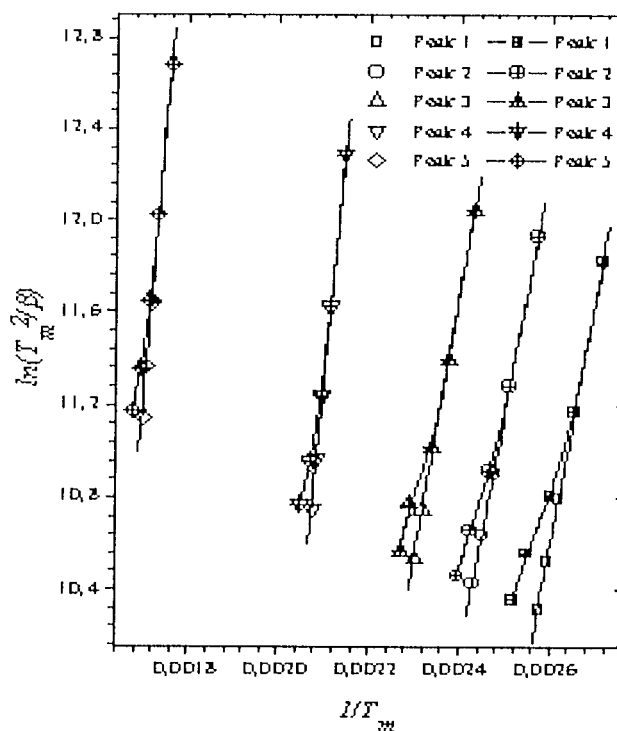
Figure 4.5: Variable heating rate plots of $ln(T_m^2/\beta)$ against $1/T_m$. In the figure, open and + centered symbols represent the calculated and experimental points after dose level 50 Gy, respectively

The all glow curves were also analyzed by CGCD method. This method has become very popular method to obtain kinetic parameters for the last two decades [20], since it has great advantages over the experimental methods (i.e. initial rise, peak shape, isothermal decay, variable heating rate and etc) owing to simultaneous determination of kinetic parameters of all peaks without no additional thermal treatments and experimental repetitions. Also, this method uses all data points in the whole glow curve rather than just a few points during the curve fitting procedures. It is apparent that if the number of data points used in the analysis increases, the potential for accurate determination of the kinetic parameters gets better. However, it must be noted that different models, approximations and minimization procedures are used for the glow curve analysis in the CGCD program. As a consequence, one may wonder whether the results of CGCD method reflect the accurate kinetic

parameters of the TL peaks. According to many experienced researchers, the results obtained by the CGCD method, in some cases, seem to be unreliable.

Especially, the advantages of the CGCD method may be undermined in complex TL glow curves. One may get a local minimum of the least square function which may yield erroneous kinetic parameters as the computerized fitting routine attempts to define the "best-fit" to the numerical data. As a result, many possible sets of kinetic parameters could be assigned to the same glow curve. The used CGCD program, which is based on the least square minimization procedure, was developed at the Reactor Institute at Delft, The Netherlands. The detail results of these models were given in an IRI-CIMAT Report [57]. In the given present study, the first-order kinetics were approximated for all CGCD evaluations by the expression,

$$I(T) = n_0 s \exp(-\frac{E}{kT}) \exp\left[(-\frac{s}{\beta} \frac{kT^2}{E} \exp(-\frac{E}{kT}) * (0.9920 - 1.620 \frac{kT}{E}) \right] \qquad (4.2)$$

and the general-order kinetics were approximated by the expression,

$$I(T) = n_0 s \exp(-\frac{E_a}{kT}) \exp\left[1 + \frac{(b-1)s}{\beta} \frac{kT^2}{E_a} \exp(-\frac{E_a}{kT})(0.9920 - 1.620 \frac{kT}{E_a}) \right]^{\frac{b}{1-b}} \qquad (4.3)$$

where n_0 (m^{-3}) is the concentration of trapped electrons at $t=0$, T (K) is the absolute temperature, k (eVK^{-1}) is Boltzmann's constant, β ($^{\circ}$Cs^{-1}) is heating rate and b is the kinetic order. The goodness of fit for all the measured glow curves was tested using the figure of merit (FOM) [58]. From many experiences, it can be said that, if the values of FOM are between 0.0% and 2.5% the fit is good, 2.5% and 3.5% is fair fit, and >3.5% is bad fit. In the analyses of the complex glow curves by CGCD method, it is very important to decide correctly how many glow peaks there are in the glow curve and which of them have first or general-order kinetics to obtain correct results.

In some cases, the best-fits can be obtained when different number of peaks is used in the CGCD analyses instead of real number of glow peaks to be in the glow curve. However, the values of kinetic parameters do not reflect their correct values when an incorrect number of glow peaks are assumed in the glow curve even if the best-fits were obtained. Therefore, firstly one must decide the number of glow peaks and their kinetic orders in the glow curve of APSQ. In the present work, after the many tries with different number of glow peaks, it was observed that the glow curve structure of this sample is well described by a linear combination of at least seven first-order glow peaks. However, the glow curve analysis yields consistent fit results for all heating rates, the results do not generally agree with each other, because the results of kinetic parameters are also highly dependent upon the input parameters such as the location of individual peaks. The parameters finally so selected were the values that yielded the best overall fit to the designated high priority features of the TL results. Figure 4.6 shows the results of CGCD fitting on the assumption of seven peaks and Table 4.1 shows the results of the best estimates of peak parameters.

No estimates of mathematical uncertainty were available with this program but the inability to differentiate clearly between quite different initial assumptions regarding the number of peaks and their peak temperatures underlines the unsuitability of CGCD for TL glow peaks of this type. This is in accord with a number of reports aldready described in section 1 which indicates that glow peaks in quartz are often best described by multible peaks with first –or general order kinetics, or a continuum of trapping energies and frequency factors.

Table 4.1 summarizes the E_a and s values as determined by the IR, VHR and CGCD methods. Comparison of E_a and s values obtained by the various methods is very complex. For the presumed peaks 1, 2 and 3, the E_a values determined by IR

and VHR methods are in reasonable agreement but not with CGCD method. The s values are always 3-4 orders of magnitude different for all methods.

In general, there were large disparities between the results of different methods for high temperature glow peaks. These are probably due to artifacts in the methods related to the large number of overlapping peaks. Because the high degree of overlap limits the accuracy of the determined parameters and therefore, the usefulness of CGCD method is reduced for the determination of kinetic parameters [59].
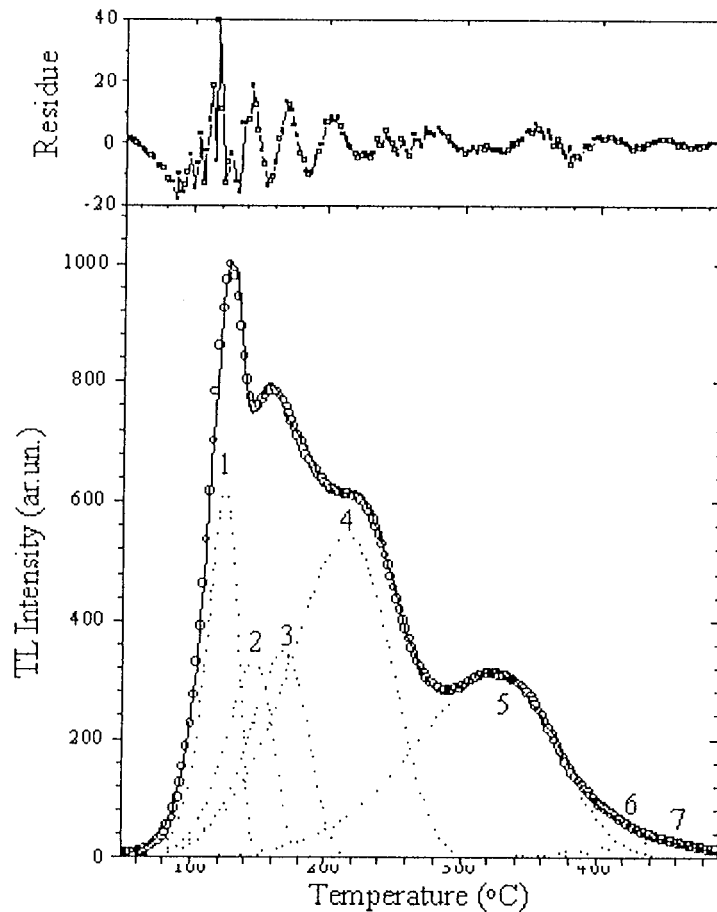

Figure 4.6: A typical analyzed glow curve of APSQ measured after ≈50 Gy irradiation at room temperature. The glow curve was measured by heating the sample to 500 °C at a heating rate of 5 °C/s. In the figure, open circles represent the experimental points

During the partial thermal annealing process, the glow peaks are gradually

narrowed with increasing partial thermal annealing temperature and time (Fig.4.2).

In addition the glow peak temperature gradually shifted to the high temperature

sides with increasing bleaching time and temperature. These behaviors suggest that

the glow curve of this sample is the combination of highly overlapped first-order

glow peaks or the kinetic orders of all peaks should have higher than first-order

kinetics. But, the second interpretation is completely contrary to the result of

additive dose method and therefore the first interpretation seems more logical than

second one. Anyway, the evaluated kinetic parameters by CGCD method are

continuously increased with increasing bleaching temperature and reach the values

determined by VHR method.

Table 4.1. The values of the activation energy E_a (eV) and frequency factor s (s^{-1}) of TL peaks of APSQ determined by the IR, VHR and CGCD methods.

Peak No	T_m (°C) (β=1 °C/s)	IR Method		VHR Method		CGCD Method	
		E_a (eV)	$ln(s)$ (s^{-1})	E_a (eV)	$ln(s)$ (s^{-1})	E_a (eV)	$ln(s)$ (s^{-1})
1	96	0.90±0.01	25.88±0.36	0.94±0.10	17.77±1.9	1.11±0.07	16.45±1.68
2	116	0.93±0.01	25.39±0.35	0.93±0.25	15.67±2.8	0.83±0.03	32.72±1.54
3	139	0.99±0.01	28.93±0.35	1.00±0.23	16.01±2.6	0.71±0.04	21.49±1.06
4	193	1.11±0.02	24.95±0.41	1.84±0.20	33.38±2.4	0.50±0.02	9.57±0.57
5	296	1.22±0.02	21.50±0.45	2.12±0.20	30.63±2.4	0.58±0.04	8.42±0.15
6	378	1.28±0.01	19.23±0.10	-	-	2.34±0.1	38.03±2.0
7	405	1.36±0.02	19.32±0.20	-	-	1.09±0.15	15.52±3.05

The dose response was also investigated by the peak height method for all

components in the glow curve of APSQ. All data in dose response are plotted on a

log-log scale and shown in Fig.4.7. It is clearly seen that the dose responses of all

components follow similar pattern and are strongly linear with slopes of ≈3, as

readily seen in Fig.4.7. The peak 1 exhibits linearity up to 5 Gy after which it

saturates at 10 Gy. On the contrary, the other peaks, peaks 2+3, 4 and 5, exhibit

linear dose responses up to 250 Gy, after which strong saturation occurs for all components.

Besides, the slope of linearity decreases with increasing temperature that means peak 1 has higher dose response than peaks 2+3 and so on (Fig.4.7). As seen also from Fig.4.7, the minimum detectable dose of unannealed APSQ is very high, i.e. greater than 1 Gy for high temperature peaks 3 and 4. However, it must be remembered that the sensitivity of all types of quartzes originating from various sources substantially increases after the annealing at 500 °C or higher temperatures for at least 1 h but it is more interesting that this process also changed the slope of dose responses of all peaks [60]. Thus, the sensitivity of annealed samples is much stronger than that of the unannealed samples and therefore minimum detectable dose levels are reduced below 1 Gy with annealing of samples at high temperatures for sufficient period. There are a number of ways to explain the increase in the sensitivity following annealing. One of them might be removal of unknown non-radiative recombination centers and the other might be the creation of additional luminescent centers [61].

The stability of the stored signal at normal temperatures is an important factor in many applications such as archaeological and geological dating, personal and environmental dosimetry, etc. Any appreciable decay in the stored signal at room temperature will invalidate the relationship between TL emitted and the radiation exposure that may have been delivered at some considerable time before readout. The extent of TL signal decay over long periods is difficult if not impossible to measure directly, particularly in archeological applications. The measured glow curves of APSQ at the end of the planned storage periods are shown in Figure 4.8. As seen from this figure, the intensity of low temperature peaks 1-3 are quickly

decreased while high temperature peaks 4-7 are not sufficiently influenced from storage periods at room temperature.
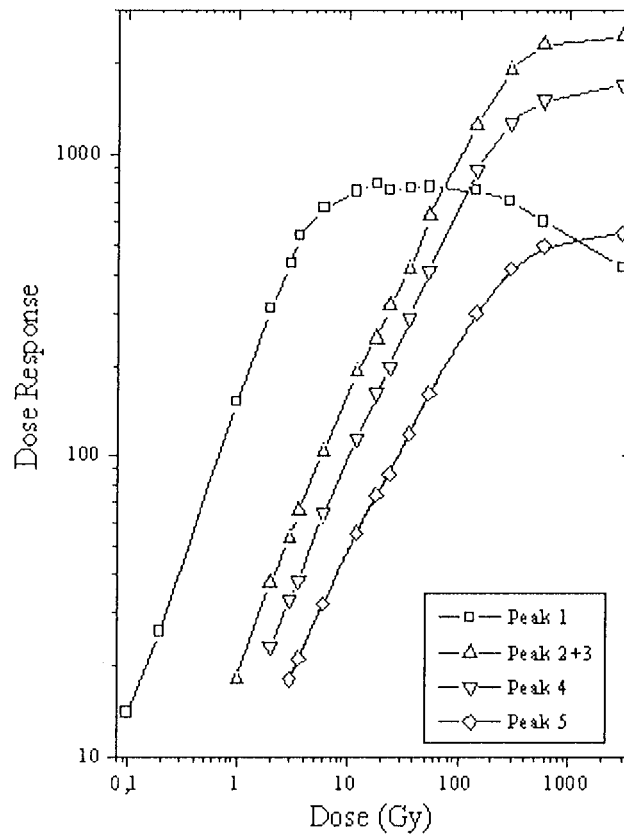

Figure 4.7: The dose response of first five peaks (P1-P5) determined by peak height method. Note that each experimental point is the average of at least four measurements

The normalized relative responses of analyzed glow peaks by CGCD method are shown in figure 4.9. Each point in the figure is the average of four readings. After the storage at room temperature for 1 month, peaks 1 and 2 were completely removed from the glow curves. The TL yield of peak 3 was reduced to typically 27% of its original value after one month at room temperature whereas peak 4 faded 10% during this period. On the other hand, any noticeable reduction was not recorded on the intensity of peaks 5-7 after one month.
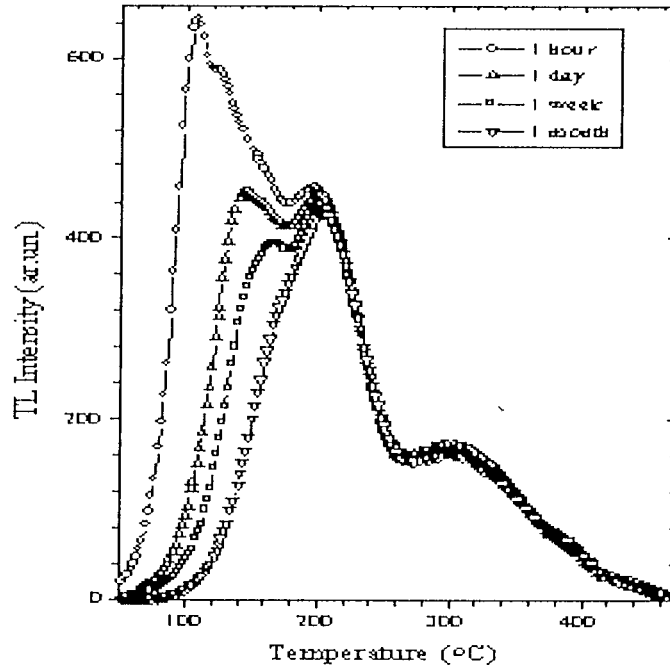
Figure 4.8: Some of the selected glow curves of APSQ recorded after planned storage periods at room temperature in the dark room
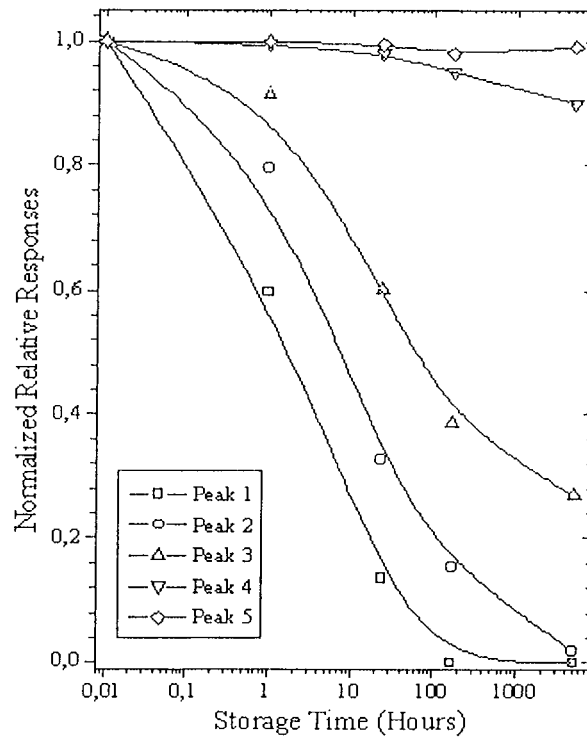

Figure 4.9: Fading evaluation of the deconvoluted peaks of APSQ at room temperature in the dark room

46

4.2. Results and discussion for CaSO$_4$

As mentioned previously (Section 4.1.), the determination of E_a and s mainly depends on the prior knowledge of b and exact number of glow peaks in the glow curve [20]. Therefore, to form an opinion about the b of individual glow peaks in CaSO$_4$:Dy, the AD method was again used. The samples were irradiated for five different dose durations between 5 mins and 60 mins using a ^{137}Cs gamma ray source to check the dose dependence effect on the peak position of each individal glow peak. It is known that this is a simple test for the first-order kinetics. The measured glow curves after different dose durations are shown in figure4.10. As seen from this figure, there is no significant change in the position of peak temperatures and they are within the experimental error ±4 °C for all the doses. This point clearly indicates that the all peaks in the glow curve of CaSO$_4$:Dy should have first-order kinetics. The result also indicate that the glow curve of CaSO$_4$:Dy in the temperature range from RT to 350 °C is seen as the superposition of six-glow peaks. However, to study the kinetic parameters of this material in detail, it is required to record the glow curves of this material after different experimental procedures. But, as mentioned before our Harshaw TLD analyser was out of order and could not be repaired during the preparation time of this thesis so CaSO$_4$:Dy samples were analysed by Toledo TLD reader in Ankara Nuclear Research and Training Center (ANAEM). All the measured glow curves with different dose levels are given in figure 4.10.

(a)
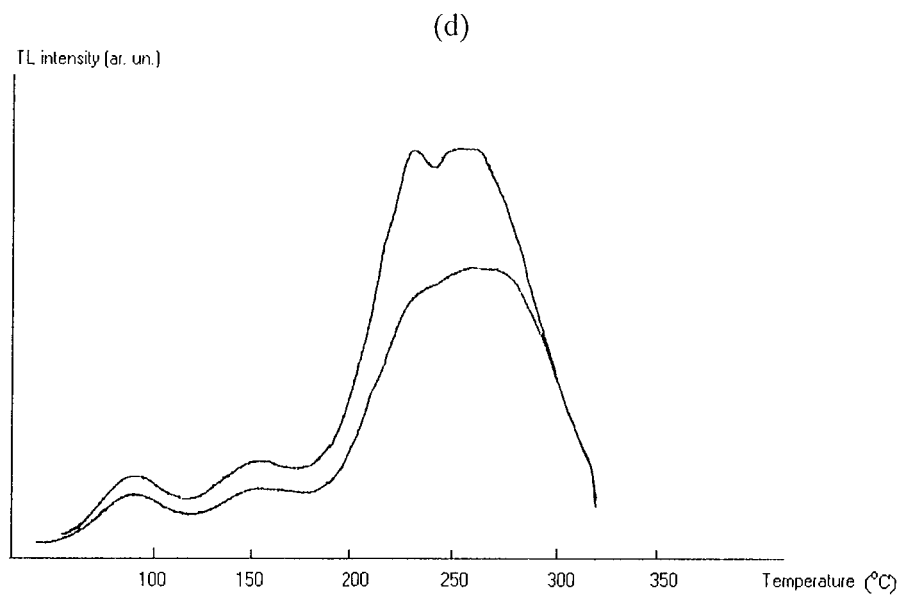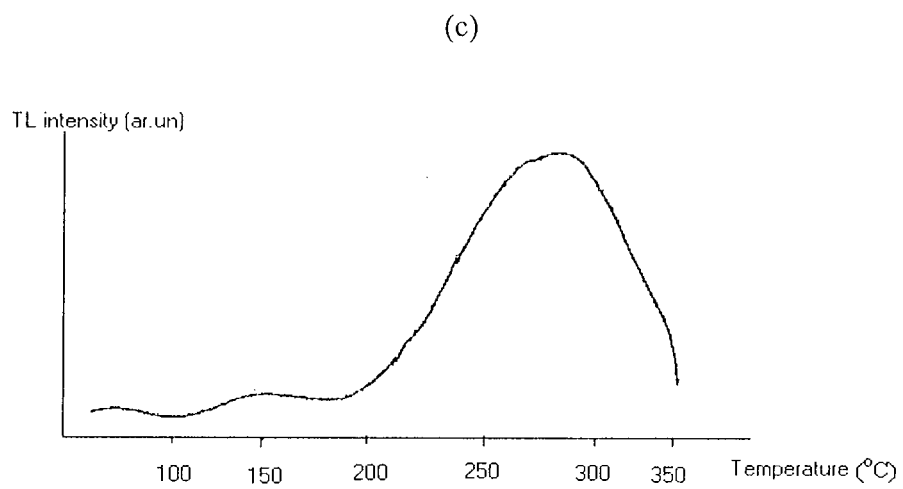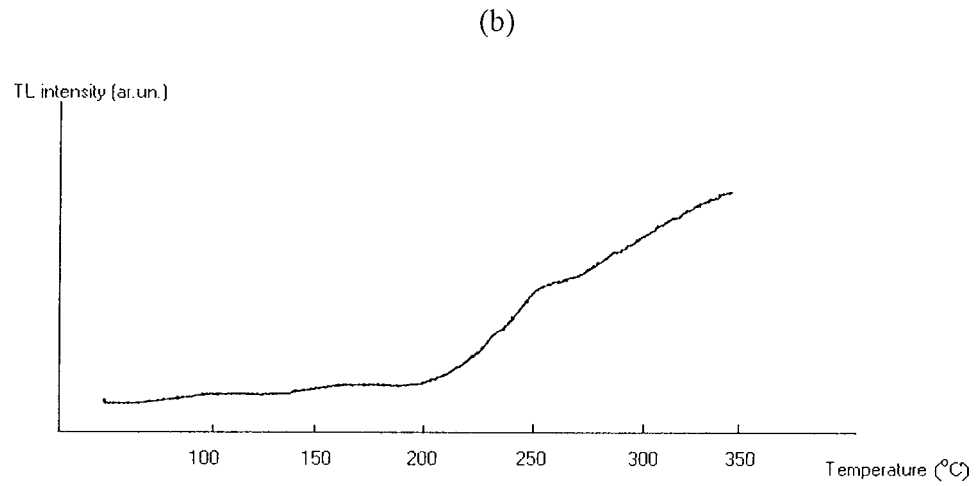

47

(b)

(c)

(d)
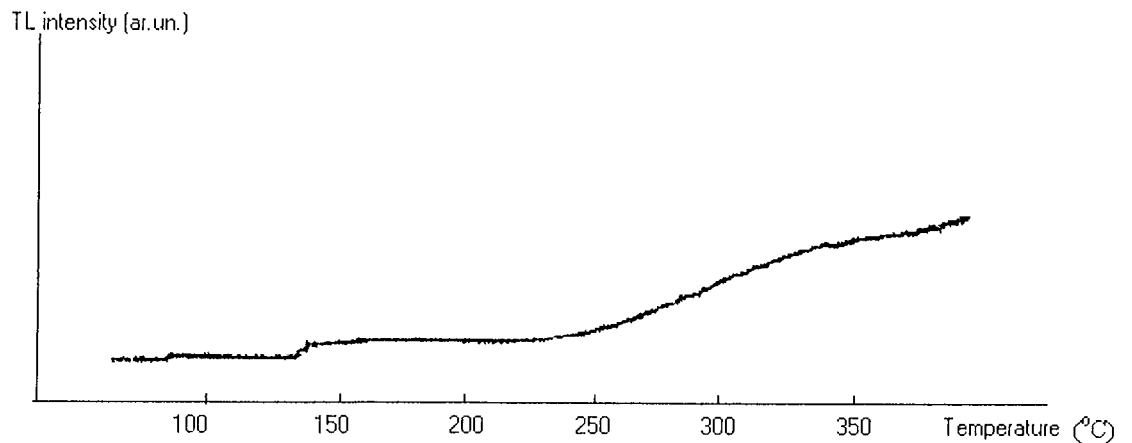
Figure 4.10: Some of the selected glow curves of CaSO$_4$:Dy with different dose levels. (a) For 5 min (8.33 mGy), (b)For 15 min (24.99 mGy), (c) For 30 min (49.98 mGy), (d) For 45 and 60 min (74.97 mGy and 100 mGy)

CHAPTER 5

CONCLUSION

The results in the present work indicate that the glow curve APSQ after beta irradiation between 0.02 and 2.5 kGy in the temperature range from room temperature to 470 °C can be best described as a superposition of seven glow peaks. Additive dose experiment indicates that all of them have first-order kinetics. The activation energies found by IR and VHR methods for peaks 1,2 and 3 yield very close values. For all other peaks (P4-P7), there is no any consensus or agreement between the results of all applied methods. However, the evaluated kinetic parameters of these peaks by CGCD method are close to the calculated values by VHR method after the application of thermal bleaching experiment.

Because the full width at half maximum of all peaks decrease with increasing temperature and the evaluated kinetic parameters of these peaks gradually increase and reach to the calculated values by VHR method during the thermal bleaching experiment. So, the determined values of kinetic parameters by VHR method without any thermal bleaching are more reliable than the determined values of CGCD method, since the last procedure often gives rise to ambiguous results due to high overlapping peaks in the glow curve. Additionally, the initial rise method gives the value of E_a, 35-45% lower than the value obtained by VHR method for peaks 4 and 5. This fact has been already analyzed by Wintle and she has showed that this discrepancy might be caused by non-radiative transitions in the luminescent centers that could lead to a computation of an apparent energy differing from the real energy by an amount W.

So, what one obtains is $(E_a\text{-}W)$ instead of E_a. It can be considered that there is no sufficient effect of thermal quenching below 200 °C. Therefore, an investigation of thermal quenching is a necassary precursor to the use of the RIR method. On the other hand, an interesting point must be noted that if the thermal quenching exists in a given material, it is expected that the TL sensitivity of this materail decraeses with increasing heating rate, which was not observed in the investigated material.

The dose responses of all components of unannealed APSQ have similar pattern, first follow strong linearity and then saturate at different dose levels. When the glow curves of this material stored in the dark room were recorded after one month, the peaks 1 and 2 were not observed, the peak 3 reduced to 27% of its original value whereas the other peaks were not sufficiently affected during this period.

It is unfortune that we are not able to present any data and make any conclusions for the kinetic parameters of $CaSO_4$ samples due to the unavailabity of the TLD-3500 reader as mentioned previously.

REFERENCES

[1]   McKeever SWS, Thermoluminescence of solids Cambridge University Press,(1985).

[2]   McKeever S W S, *Radiat. Prot. Dosim.*, **8**, 81 (1984).

[3]   Aitken M J, "*Thermoluminescence Dating*", Academic Press, London, (1985).

[4]   Othman I E and Charles M W, *Radiat. Prot. Dosim.*, **84**, 193 (1999).

[5]   Chen R, Yang X H and McKeever S W S, *J. Phys. D: Appl. Phys.*, **21**, 1312 (1988).

[6]   Martini M, Spinola G and Vedda A, *Radiation Effects*, **105**, 185 (1997).

[7]   Jani M G, Halliburton L E and Kohnke E E, *J. Appl. Phys.* **54**, 6321 (1984).

[8]   Petrov S A and Bailiff I K, *Radiat. Meas.*, **24**, 519 (1995).

[9]   Hornyak W F, Chen R and Franklin A, *Phys. Rev. B*, **46**(13), 8036 (1992).

[10]   David M, Kathuria S P and Sunta C M, *Ind. J. Pure Appl. Phys.*, **20**, 519 (1982).

[11]   Petrov S A and Bailiff I K, *Radiat. Meas.*, **27**, 185 (1997).

[12]   Hwang F S W, *J. Geophys. Res.*, **77**, 328 (1972).

[13]   Mattern P L, Lengweiler K and Levy P W, *Radait. Eff.*, **26**, 237 (1975)

[14]   Schwartzman R G, Kiersted J A and Levy P W, *PACT*, **9**, 163 (1983).

[15]   West R H and Carter A C, *Radiat. Eff. Lett.*, **57**, 129 (1980).

[16]   Prokein J and Wagner G A, *Radiat. Meas.*, **23**, 85 (1994).

[17]   Kitis G, Pagonis V, Carty H and Tatsis E, *Radiat.Prot.Dosim.*, **100**, 225 (2002).

[18]   Pagonis V, Tatsis E, Kitis G, Drupieski C, *Radiat.Prot.Dosim.*, **100**, 373 (2002).

[19]   Chen R and McKeever S W S, *Theory of Thermoluminescence and Related Phenomena*, World Scientific,Singapore,(1997).

51

[20] Horowitz Y S and Yossian D, *Radiat.Prot.Dosim.*, **60**, 1 (1995).

[21] J.K.Srivastava, B.C. Bhatt and S.J. Supe, *Radiat.Prot.Dosim.*, **40**, 271 (1992).

[22] T.Yamashita, T., Nada, N., Onishi, H., and Kitumura, *Healt Phys.,* 21,295 (1971).

[23] Yigal and Horowitz, *Thermoluminescence and Thermoluminescent Dosimetry*

[24] Portal G.,*Aplied Thermoluminescence Dosimetry*, **97**, (1979)

[25] J.K. Srivastava and S.J. Supe, *J.Phys. D* **13** (1980)

[26] B.Bunghkbardt, D. Singh and E.Piesch, *Nuclear Instrumentations and Methods*, **142**, (1977)

[27] F. Daniels, C.A. Boyd and D.F. Saunders *Science* **117**, 343, (1953)

[28] P.D. Townsend and J.C. Kelly, Colour Centres and Imperfections in Insulators and Semiconductors, Sussex University Press, London, (1993).

[29] McKeever SWS, M. Moscovitch and P.D. Townsend *Thermoluminescence Dosimetry Materials: Propeties and Uses*, Nuclear Technology Publishing, Kent (1995).

[30] R. Chen and McKeever SWS, *Theory of Thermoluminescence and Related Phenomena*, World Scientific, Singapore (1997).

[31] J.T. Randall and M.H.F. Wilkins *Proc.R.Soc.London Ser. A* **184**, 366, (1945).

[32] J.T. Randall and M.H.F. Wilkins *Proc.R.Soc.London Ser. A* **184**, 390, (1945).

[33] R. Chen, in: Y.S. Horowitz (Ed.), Thermoluminescent and Thermoluminescent Dosimetry, Vol. 1, CRC Press, Boca Raton, FL, (1984).

[34] G. Kitis, J.M. Gomez-Ros and J.W.N. Tuyn *J.Phys.D:Appl.Phys.* **31**, 2636, (1998).

[35] R.V. Pagonis, S.M. Mian and G. Kitis *Radiat.Protect.Dosim.* **93**, 11, (2001).

[36] G.F.J. Garlick and A.F. Gibson *Proc.Phys.Soc.* **60**, 574, (1948).

[37] A.J.J. Bos and J.B. Dielhof *Radiat.Prot.Dosim.* **36**, 231, (1991).

[38] C.E. May and J.A. Partridge *J.Chem.Phys.* **40**, 1401, (1964).

[39] P.J. Kelly, M.J. Laubitz and P. Bräunlich *Phys.Rev.B* **4**, 1960, (1971).

[40] Chen and A.A. Winer *J.Appl.Phys.* **41**, 5227, (1970).

[41] T.M. Piters and A.J.J. Bos *J.Phys.D:Appl.Phys.* **26**, 2255, (1993).

[42] Chen R *J.Appl.Physics* **40**, 570, (1969).

[43] Grossweiner L I *J.Appl.Physics* **24**, 1306, (1953).

[44] Halperin A and Braner A A *Phys.Rev.* **117**, 405, (1960).

[45] Booth A H *Can. J.Chem.* **32**, 214, (1954).

[46]   Azerin J *Nucl.Tracks* **11**, 159, (1986).

[47]   Kathuria S P and Sunta C M *J.Phys.D:Appl.Phys.* **12**, 1573, (1979).

[48]   Bos A J J, Piters J M, Gomez Ros J M and Delgado A (GLACANIN, and Intercomparision of Glow Curve Analysis Computer Programs) IRI-CIEMAT Report 131-93-005 IRI Delft (1993).

[49]   Mahesh K, Weng P S and Furetta C, *Thermoluminescence in Solids and its Applications*, (Nuclear Technology Publishing Ashford) (1989).

[50]   Hsu P C and Wang T K *Radiat.Protect.Dosim.* **16**, 253 (1986).

[51]   Sunta C M *Radiat.Protect.Dosim.* **8**, 25, (1984).

[52]   McKeever S W S, Moscovitch M and Townsend P D, *TL Dosimetry Materials: Properties and Uses*, (Nuclear Technology Publishing Ashford) (1995).

[53]   Kirsh Y, *Phys. Stat. Sol.* A, **129**, 12 (1992).

[54]   Christodoulides C, *J. Phys. D:Appl. Phys.*, **18**, 1665 (1985).

[55]   Singh T S C, Mazumdar P S and Gartia R K, *J.Phys.D:Appl.Phys.*, **21**, 1312 (1988).

[56]   Kitis G and Tuyn J W N, *J. Phys.D:Appl.Phys.* **31**, 2065 (1998).

[57]   Bos A J J, Piters J M, Gomez Ros J M and Delgado A, (GLOCANIN, and Intercomparision of Glow Curve Analysis Computer Programs) IRI CIEMAT Report,131-93-005 IRI Delft (1993).

[58]   Misra S K and Eddy N W, *Nucl. Instrum. Methods* **166**, 537 (1979).

[59]   Yazici A N, *Radiat.Prot.Dosim.*, submitted by journal.

[60]   Charitidis C, Kitis G, Furetta C and Charalambous S, *Nucl. Instrum. Meth. B*, **168**, 404 (2000).

[61]   Kristianpoller N, Abu-Rayya M and Chen R, *Radiat.Prot.Dosim.*, **33**, 193 (1990).